JBC RESEARCH ARTICLE

The yeast mitochondrial succinylome: Implications for regulation of mitochondrial nucleoids

Received for publication, February 24, 2021, and in revised form, August 23, 2021 Published, Papers in Press, September 1, 2021,
https://doi.org/10.1016/j.jbc.2021.101155

Jan Frankovsky[1,‡], Barbora Keresztesová[2,‡], Jana Bellová[3], Nina Kunová[2], Nikola Čanigová[1], Katerina Hanakova[4], Jacob A. Bauer[2], Gabriela Ondrovičová[2], Veronika Lukáčová[5], Barbara Siváková[3], Zbynek Zdrahal[4], Vladimír Pevala[2], Katarína Procházková[1], Jozef Nosek[6], Peter Baráth[3,5,*], Eva Kutejova[2,*], and Lubomir Tomaska[1,*]

From the [1]Department of Genetics, Comenius University in Bratislava, Faculty of Natural Sciences, Bratislava, Slovakia; [2]Institute of Molecular Biology and [3]Institute of Chemistry, Slovak Academy of Sciences, Bratislava, Slovakia; [4]Central European Institute of Technology (CEITEC), Masaryk University, Brno, Czech Republic; [5]Medirex Group Academy, Trnava, Slovakia; and [6]Department of Biochemistry, Comenius University in Bratislava, Faculty of Natural Sciences, Bratislava, Slovakia

Edited by John Denu

Acylation modifications, such as the succinylation of lysine, are post-translational modifications and a powerful means of regulating protein activity. Some acylations occur non-enzymatically, driven by an increase in the concentration of acyl group donors. Lysine succinylation has a profound effect on the corresponding site within the protein, as it dramatically changes the charge of the residue. In eukaryotes, it predominantly affects mitochondrial proteins because the donor of succinate, succinyl-CoA, is primarily generated in the tricarboxylic acid cycle. Although numerous succinylated mitochondrial proteins have been identified in *Saccharomyces cerevisiae*, a more detailed characterization of the yeast mitochondrial succinylome is still lacking. Here, we performed a proteomic MS analysis of purified yeast mitochondria and detected 314 succinylated mitochondrial proteins with 1763 novel succinylation sites. The mitochondrial nucleoid, a complex of mitochondrial DNA and mitochondrial proteins, is one of the structures whose protein components are affected by succinylation. We found that Abf2p, the principal component of mitochondrial nucleoids responsible for compacting mitochondrial DNA in *S. cerevisiae*, can be succinylated *in vivo* on at least thirteen lysine residues. Abf2p succinylation *in vitro* inhibits its DNA-binding activity and reduces its sensitivity to digestion by the ATP-dependent *Sc*Lon protease. We conclude that changes in the metabolic state of a cell resulting in an increase in the concentration of tricarboxylic acid intermediates may affect mitochondrial functions.

Mitochondria are semiautonomous organelles that must be flexible in their responses to changes in both extracellular and intracellular conditions. Mitochondrial functions, from basal metabolism to communication with other cellular compartments, are regulated on several levels (1–3). One of the most dynamic ways to affect the activity of proteins and nucleic acids is to add small chemical groups. For proteins, these modifications occur mostly post-translationally and are called post-translational modifications (PTMs).

The most studied PTM is phosphorylation catalyzed by protein kinases (4). Although the number of protein kinases localized to the yeast mitochondria does not seem to be high (5–7), an analysis of the mitochondrial phosphoproteomes of numerous eukaryotes, including the yeast *Saccharomyces cerevisiae*, revealed that mitochondrial proteins are relatively frequently phosphorylated (6–12). In addition to phosphate, many other chemical groups can be attached to the side chains of amino acids. In mitochondria, the most frequent PTM is the acylation (*e.g.*, acetylation, propionylation, malonylation, glutarylation, succinylation) of lysine residues (13). Acyl groups are donated by the corresponding acyl-CoA, whose concentration is particularly high in mitochondria (14, 15). Moreover, the higher intramitochondrial pH favors the deprotonation of the lysine epsilon amino group, thus increasing its nucleophilicity and reactivity (13). Mitochondrial acylation is mostly nonenzymatic and is driven by increases in acyl-CoA concentration (16, 17).

The properties of the modified lysine are most dramatically changed by its malonylation, glutarylation, and succinylation, that is, acylations that change the charge of the affected residue. Succinylation of lysine results in the formation of 6-*N*-succinyl-L-lysine (Ksucc). Lysine succinylation was first shown to affect the active site of the *Escherichia coli* homoserine *trans*-succinylase (18); later, it became clear that succinylation is a frequently occurring PTM in both prokaryotes and eukaryotes (19, 20). Succinylation is particularly interesting in terms of mitochondrial regulation because the concentration of succinyl-CoA within the mitochondria varies significantly depending on the activity of the enzymes involved in the tricarboxylic acid (TCA) cycle (13, 19).

The succinylation of mitochondrial proteins is not only affected by natural physiological changes but can also be changed by mutations that cause changes in cellular metabolism. For example, the dominant mutations that occur in the

‡ These authors contributed equally to this work.
* For correspondence: Peter Baráth, chempeto@savba.sk; Eva Kutejova, eva.kutejova@savba.sk; Lubomir Tomaska, lubomir.tomaska@uniba.sk.
Present address for Nikola Čanigová: Institute of Science and Technology Austria, Klosterneuburg, Austria.

genes encoding the NADP-dependent isocitrate dehydrogenases in some types of cancers (21) yield enzymes with altered substrate specificity, which catalyze the NADPH-dependent formation of 2-hydroxyglutarate (2HG) rather than the conversion of isocitrate to α-ketoglutarate (α-KG) (22). The increased concentration of 2HG in the affected cells leads to the inhibition of several key enzymes, including succinate dehydrogenase, which results in an increased concentration of succinyl-CoA (23). Because the addition of glycine, which channels conversion of 2HG into porphyrin, or the overexpression of the desuccinylase SIRT5 slows down the growth of tumor cells, it seems likely that succinylation plays a role in tumorigenesis (23).

There are numerous studies describing the cellular succinylome in a wide variety of prokaryotic and eukaryotic species (*e.g.*, (19, 24–45)). In yeast, the pioneering analysis of Weinert *et al.* (19) provided the first glimpse into the succinylome of *S. cerevisiae* and showed that the succinylation of cellular proteins is affected by the growth conditions and genetic backgrounds that affect the concentration of succinyl-CoA. One of their conclusions was that "succinylation on abundant proteins occurs at a low level and that many succinylation sites remain unidentified". As mitochondria are thought to be lysine succinylation hot spots, the proteins primarily affected by succinylation can naturally be expected to be the mitochondrial ones. However, with few exceptions (24, 43), most studies on eukaryotic succinylomes were performed on whole-cell extracts. This does provide a global picture of protein succinylation, but it may fail to detect some of the less-abundant protein targets specifically localized to distinct cellular compartments. To gain better insight into the yeast mitochondrial succinylome, we performed an MS analysis of proteins isolated from purified *S. cerevisiae* mitochondria, and we enriched the proportions of succinylated peptides by immunoprecipitating them with antibodies raised against Ksucc. We detected 314 succinylated mitochondrial proteins and identified 1763 novel succinylation sites. In particular, we found that the majority of the protein components of the mitochondrial nucleoid (mt-nucleoid), which consists of the mitochondrial DNA (mtDNA) compacted into a nucleoprotein structure, are succinylated *in vivo*. We also demonstrated that the succinylation of Abf2p, the principal component of the *S. cerevisiae* mt-nucleoid, inhibits its DNA-binding activity and reduces its sensitivity to the action of the mitochondrial ATP-dependent protease *Sc*Lon (Pim1p) *in vitro*. Finally, we discuss how changes in the concentration of succinyl-CoA can alter the compaction of mtDNA and thus might affect the biogenesis of mitochondrial respiratory complexes.

Results

Mitochondrial succinylome of S. cerevisiae

To carry out a comprehensive analysis of the *S. cerevisiae* mitochondrial succinylome in cells grown on a non-fermentable carbon source (glycerol + ethanol), we purified their mitochondria and prepared mitoplasts lacking the outer mitochondrial membrane and the proteins associated with the intermembrane space. To ensure that the sample to be analyzed by MS would contain a detectable proportion of the less-abundant succinylated proteins, we enriched the proportion of succinylated peptides by immunoprecipitating them with an anti-Ksucc antibody. To increase the number of identified succinylation sites in the WT mitoplasts, we also performed an anti-Ksucc immunoprecipitation (IP) experiment using mitoplasts isolated from a *lsc1*Δ strain. Disruption of Lsc1p, a succinyl-CoA ligase, leads to an approximate 3-fold increase in overall protein succinylation (19), allowing a larger set of modified peptides to be identified. The results of this experiment served as a template for identifying minor modified peptides in the WT strain using MaxQuant's 'match-between-runs' feature. Of 1436 identified protein groups (Table S1, protein groups), 865 were categorized as mitochondrial proteins (Table S2*A*), 314 of which were succinylated on at least one lysine residue (Table S2*B*). The number of different Ksucc sites within a single protein group ranged from 1 (91 protein groups) to 44 (the group containing aconitase (Aco1)) (Fig. 1, Table S2*B*). The identified Ksucc sites and the respective protein groups have been compared with the succinylome identified by Weinert *et al.* (19) and acetylome identified by Henriksen *et al.* (46), either globally or with respect to mitochondrial localization (Fig. 2, Table S1*F*). Our dataset contains 1763 novel Ksucc sites, 236 of which were shown to be acetylated, as well (46).

Protein structural determinants of lysine succinylation

To date, no protein lysine succinyltransferase or desuccinylase has been found in yeast mitochondria, nor has any

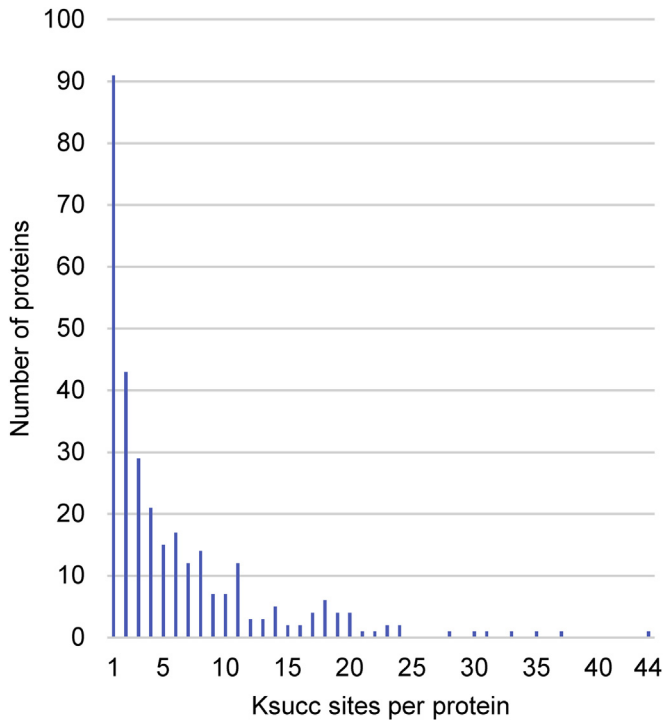

Figure 1. Number of Ksucc sites per protein. The succinylated mitochondrial proteins identified in this study were sorted according to the number of Ksucc sites per protein group. Ksucc, 6-*N*-succinyl-L-lysine.

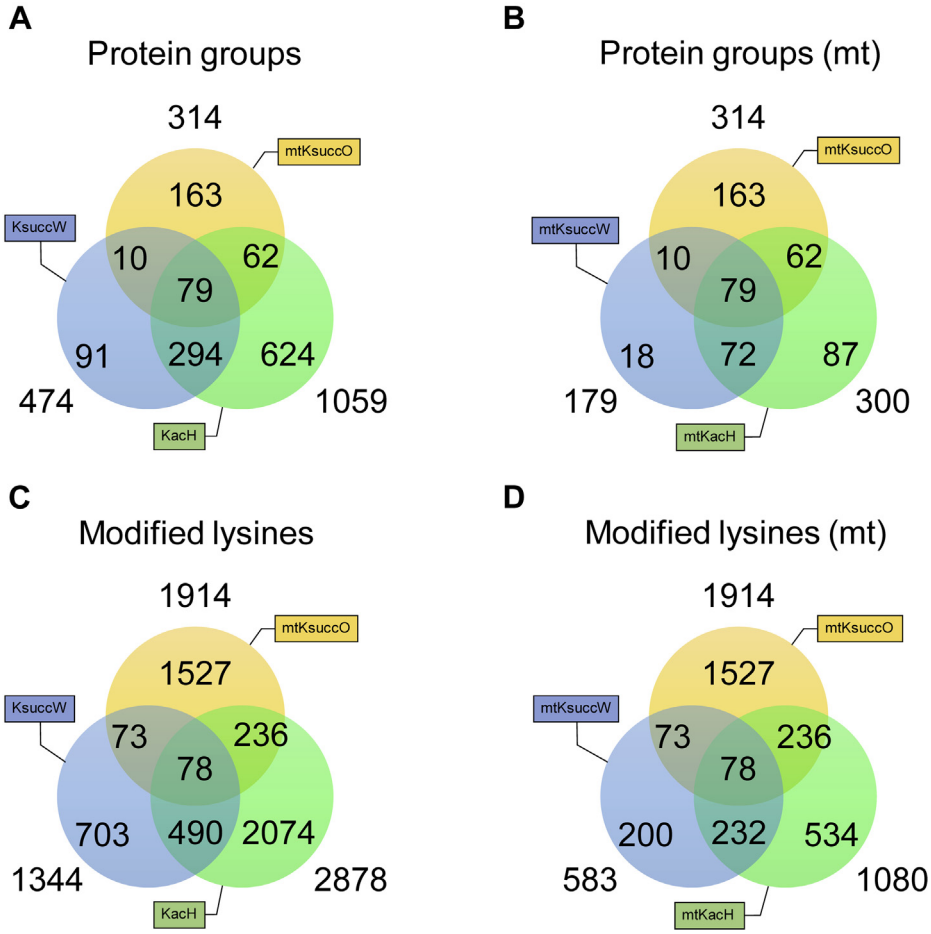

Figure 2. Protein lysine acylation dataset comparison. Acyl-modified protein groups (*A* and *B*) or sites (*C* and *D*) identified in this study (mtKsuccO) were compared with succinylome data of Weinert *et al.* (19) ((mt)KsuccW) and acetylome data of Henriksen *et al.* (46) ((mt)KacH). Comparison was general (*A* and *C*) or of mitochondrial proteins groups/sites only (*B* and *D*). Positions of acylation sites were unaccounted for within the protein group overlap analyses. Ksucc, 6-*N*-succinyl-L-lysine.

distinct sequence motif been identified. Indeed, as shown in Figure S1, it seems that no such motif exists. Because yeast mitochondrial succinylation is likely to proceed non-enzymatically, with succinyl-CoA serving as the primary donor of the succinyl group, the secondary structural context of the modified residue might have an impact on the likelihood of succinylation (17, 20, 47). To explore this hypothesis, NetSurfP-2.0 (48) was used to predict the structural characteristics of all succinylated (Ksucc) and nonsuccinylated lysines (non-Ksucc) found in this study and these were compared

Table 1
Protein structural determinants of lysine succinylation

Parameter	Value non-Ksucc (n = 7044)	Value Ksucc (n = 1908)	Value Ksucc (mt) (n = 1331)	*p*-value Ksucc	*p*-value Ksucc (mt)
Surface accessibility (relative)	0.516076	0.524961	0.521774	2.27E-02	2.00E-01
Helix (q3)	**0.445350**	**0.521543**	**0.507872**	**2.25E-11**	**2.95E-06**
Sheet (q3)	0.114046	0.106577	0.117029	2.62E-01	7.07E-01
Coil (q3)	**0.440603**	**0.371880**	**0.375099**	**1.63E-11**	**3.88E-08**
3_{10} helix (q8)	0.038865	0.035246	0.035238	1.56E-01	2.37E-01
α-helix (q8)	**0.404213**	**0.485332**	**0.472161**	**1.90E-12**	**4.73E-07**
π-helix (q8)	0.003918	0.003664	0.003419	7.18E-01	5.73E-01
β-bridge (q8)	0.006241	0.006129	0.006593	8.32E-01	5.94E-01
Extended strand (q8)	0.107690	0.099686	0.109870	2.21E-01	7.80E-01
Bend (q8)	0.067766	0.070762	0.072459	4.00E-01	2.61E-01
H-bonded turn (q8)	0.099616	0.094841	0.097013	2.99E-01	6.38E-01
Coil (q8)	**0.271690**	**0.204339**	**0.203246**	**9.54E-18**	**3.86E-14**
ϕ angle	−78.512599	−77.455463	−77.554781	8.26E-02	1.87E-01
ψ angle	**26.115213**	**17.358207**	**20.789474**	**6.22E-06**	**1.97E-02**
Disorder	**0.125166**	**0.059944**	**0.055479**	**1.18E-36**	**4.30E-33**

NetSurfP-2.0 was used to predict a probability value (or angular value) for each lysine within all proteins with at least one Ksucc site identified in this study. The average values for all lysines that were not found to be succinylated (value non-Ksucc) were compared with the average values for all lysines that were found to be succinylated (value Ksucc) and to all lysines that were found to be succinylated in the mature forms of the proteins (*i.e.*, without the MTS, which were predicted using TargetP-2.0 (value Ksucc (mt))). *p*-values are listed. A significance threshold of $p < 0.05$ was used, and statistically significant categories are in bold. Surface accessibility was statistically significant in the "Ksucc" category only.

(Table 1). Ksucc sites were found to be significantly more abundant in α-helical regions, whereas their presence in coiled and disordered regions was clearly lower. Reflecting this, the average psi (ψ) angle for Ksucc sites also shows a slight decrease (in the direction of the right-handed α-helix region of the Ramachandran plot (49)) for succinylated residues. Acylation was previously predicted computationally to have the potential to disrupt α-helices, with a consequent effect on enzyme activity (17, 20). To account for possible biases in these characteristics introduced by including the mitochondrial targeting sequences (MTSs), which are normally cleaved upon protein import to mitochondria, the predictions, the analyses, and the statistical tests were also performed using only the Ksucc sites from the regions present in the cleaved mature proteins (the MTSs were predicted by TargetP-2.0 (50)). Apart from the surface accessibility category, the differences between the Ksucc and non-Ksucc characteristics remained statistically significant. Surface exposure is an intuitive predictor of nonenzymatic modification (47), but our data do not confirm its role in mitochondrial lysine succinylation. The most pronounced difference between the Ksucc and non-Ksucc residues was their presence in disordered regions: the likelihood of finding a succinylated lysine was more than 2-fold lower than finding a nonsuccinylated lysine (Table 1). Interestingly, lysine N6-acetylation, unlike some other PTMs, was not found to be correlated with sequence (dis)order (51). Intrinsically disordered proteins and protein regions are known to be involved in the regulation of many processes, including protein–protein and protein–nucleic acid interactions and in protein degradation (for a review, see (52)), but the case for lysine succinylation remains open.

Gene ontology analysis of succinylated proteins

Gene ontology (GO) analysis of succinylated proteins using the PANTHER classification system revealed that components of some of the mitochondrial complexes exhibit >2-fold enrichment. These include respiratory chain complexes (2.13-fold), oxidoreductase complexes (2.26-fold), and mt-nucleoid (2.36-fold). The latter was chosen for a more detailed analysis as (i) it contains a distinct set of well-defined protein subunits (53), (ii) its *in vivo* properties can be assessed by a direct visualization by means of fluorescence microscopy, (iii) its principal component, the DNA-binding protein Abf2, contains multiple lysine residues that are potential targets of succinylation, (iv) the effect of succinylation on biochemical properties of Abf2p can be monitored by DNA-binding assays *in vitro*, and (v) changes in DNA-binding properties of Abf2p were shown to correlate with the state of mt-nucleoid.

The possibility that PTMs can play a role in regulation of bacterial and mt-nucleoids has already been discussed elsewhere (54, 55). To test the hypothesis that succinylation may play a role in regulation of mt-nucleoids in *S. cerevisiae*, we first checked whether a subset of the succinylated mitochondrial proteins is GO-enriched for a biological process, cellular component, or molecular function linked to mtDNA metabolism. A GO overrepresentation test for cellular component using PANTHER did give a statistically significant result for "mt-nucleoid" (raw p-value <0.001, FDR <0.01). However, our experimental procedure (enrichment of Ksucc followed by MS) is likely to be biased toward more abundant proteins, as was demonstrated previously (19). Thus, it is not clear whether this result arises because mt-nucleoid proteins are more frequently succinylated or because the mt-nucleoid proteins are among the most abundant ones in the mitochondria. The proteins associated with the dominant mitochondrial processes also suffer from the same problem (data not shown). This problem might be alleviated by leaving out the Ksucc enrichment step, but without this step, the succinylated peptides are too scarce for reliable measurements.

To address this issue, we calculated the ratio between the identified Ksucc sites divided by the total number of lysine residues in each protein (Ksucc/K) and the median abundance of each protein given in the meta-analysis by Ho *et al.* (56). Ksucc/K of the mitochondrial proteins ranged from 1 (inhibitor of F_1F_O-ATPase Inh1) to 0 (no Ksucc site detected). The results for each protein with at least one Ksucc site are plotted in Figure 3. Normalizing this number by the number of

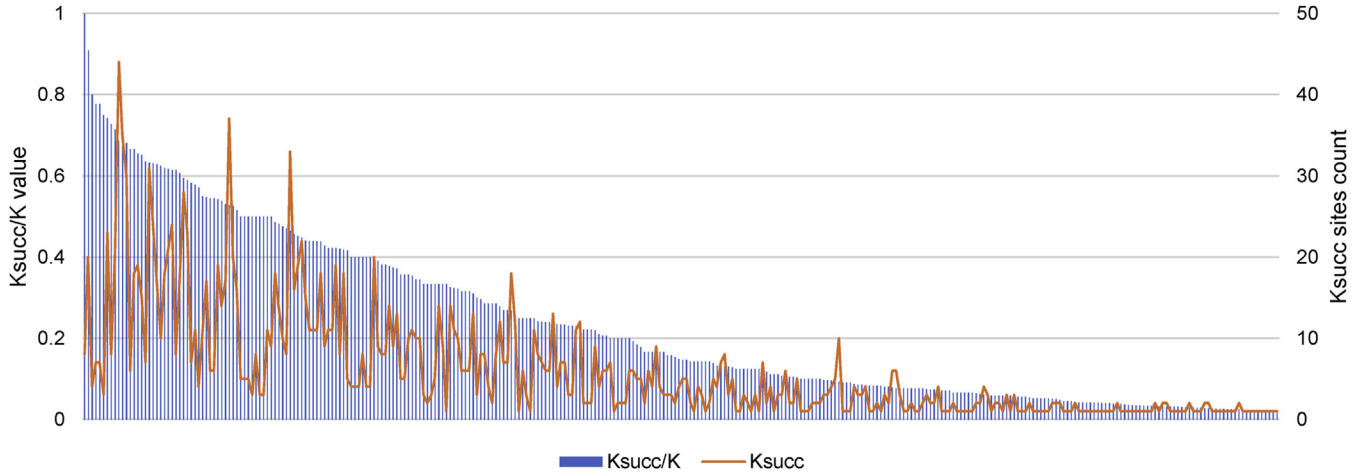

Figure 3. Plot of Ksucc site abundance in succinylated proteins. The value of Ksucc site-per-lysine (Ksucc/K) is plotted for all succinylated mitochondrial proteins identified in this study. The total number of Ksucc sites for each protein is displayed as well. Ksucc, 6-*N*-succinyl-L-lysine.

molecules per cell should allow us to distinguish between those proteins that were detected to be highly succinylated because they are frequently succinylation targets and those proteins that were detected to be highly succinylated simply because they are present in great abundance. Of the mt-nucleoid proteins, the subunits of α-KG dehydrogenase, Kgd2p and Kgd1p, have the highest Ksucc/K to molecules-per-cell ratio (see Fig. S2 for a scatter plot). With a moderate molecules-per-cell count (6516 and 11221, respectively; the median of the Ksucc proteins is 5911) (56) and a relatively high number of lysines (43 and 70, respectively; the median of the Ksucc proteins is 26), this observation is less likely to be biased. In general, the average Ksucc/K to molecules-per-cell ratio of the mt-nucleoid proteins is not higher than that of an average mitochondrial succinyl-protein (Figs. S2 and S3). Importantly, of the 24 annotated mt-nucleoid proteins, only 3 (Cha1p, Rpo41p, and Sls1p) had no detectable Ksucc sites.

Effect of succinylation on mitochondrial HMG box protein Abf2

The fact that most mt-nucleoid proteins are succinylated prompted us to investigate the possible functional consequences of this PTM on mt-nucleoid characteristics. Most of the proteins known to associate with the mt-nucleoid are bifunctional (53, 57), so assessing the effect of their succinylation on mt-nucleoid-related functions is rather difficult. One protein that is mainly dedicated to compacting the mtDNA into the mt-nucleoid in *S. cerevisiae* is Abf2p, a mitochondrial high-mobility group box (HMG box) containing protein (mtHMG protein) that binds and bends mtDNA into higher-order structures (54). The previous proteomic study (19) identified a single succinylated lysine (K162) in Abf2p. We found twelve additional succinylated lysines distributed along the entire protein, but most of them occurred within its two HMG boxes (Fig. 4*A*). Specifically, as seen in Figure 4*B*, one of the Ksucc residues is found in the N-helix and six are found in each HMG box. It can also be seen that the second Ksucc in each box is separated from the first by 12 residues, although superimposing HMG box 2 on HMG box 1 does not show them to be structurally equivalent. This superposition does show that K80, K91, and K98 from HMG box 1 are structurally equivalent, respectively, to K153, K164, and K171 from HMG box 2. The succinylation sites are all found on the outer, convex surface of Abf2p; with the possible exception of K162, none are found on the concave, DNA-binding inner surface (Fig. 4*C*). Five of these residues (K40, K63, K98, K105, and K171) have *in vitro*–modified/–unmodified ratios of more than 0.25 (Table S3) and are also known to be succinylated *in vivo*; consequently, an Abf2p carrying Ksucc at these five locations might plausibly be expected to exist *in vivo*. Calculating the electrostatic surface area shows that the replacement of these five lysine residues with succinyllysine has a modest effect on the electrostatic potential of the protein. As seen in Figure 4, *D* and *E*, unsuccinylated Abf2p has a strongly positively charged surface, with an overall charge of +12 e, whereas the replacement of these five residues reduces the positive charge on the surface to only +5 e and leaves the DNA-binding cleft largely unchanged. If all 13 lysines were to be succinylated, the overall surface charge would actually become negative, −1 e. It should be noted here, however, that there is presently no data showing that all 13 succinylations occur at one time on a single molecule.

K162, the previously identified Abf2p succinylation target (19), was also shown to interact with the DNA backbone (58), being the only one of the succinylation targets to do so. Although the remaining succinylated lysine residues do not appear to directly interact with the DNA backbone, they are close to some that do. In particular, K40 is close to K44 and R45, R69 is close to the succinylated K75, W81 is next to K80, K89 (not succinylated in the IP experiments) is close to K91 (which is), and I150 and W154 flank K153. Overall, it appears that succinylation of Abf2p is unlikely to prevent DNA binding sterically but is likely to disfavor it electrostatically.

To test the effect of Abf2p succinylation on its DNA-binding properties, we succinylated recombinant Abf2p *in vitro* using succinyl-CoA as a succinyl group donor and found that it inhibited the DNA-binding activity of the protein in both a time- and concentration-dependent manner (Fig. 5, *A* and *B*). The incomplete inhibition may be due to unequal succinylation of the Abf2p molecules present in the reaction mixture and/or affecting dissociation constant of Abf2p to the dsDNA probe. The fact that the effect of succinylation on DNA binding starts to be apparent at concentrations of succinyl-CoA higher than 1 mM is in agreement with the physiological concentrations of this acyl-CoA (14, 15). We also found that the inhibition of Abf2p's DNA-binding is not caused simply by the mere presence of succinyl-CoA in the reaction mixture but is due to the actual modification of the protein (Fig. S4*A*). In addition, incubating Abf2p with DNA before the succinylation reaction did not affect the inhibitory effect of succinyl-CoA on its DNA-binding activity (Fig. S4*B*), indicating that, at least *in vitro*, the binding of Abf2p to DNA does not prevent its succinylation. The MS analysis of Abf2p succinylated *in vitro* revealed that the majority of the lysines are modified, including those identified in our immunoprecipitated samples (see the legend to Fig. 4*A*).

As Abf2p and its orthologs from several fungal pathogens (including Gcf1p of *Candida albicans*) were shown to have several acetylated lysine residues (49, 59), we tested whether acetylation also inhibits the DNA-binding activity of Abf2p. To this end, we incubated purified Abf2p with 10 mM acetyl-CoA or 10 mM acetylphosphate, which were shown to be acetyl group donors in nonenzymatic reactions *in vitro* (60, 61). We observed that, in contrast to succinyl-CoA, preincubation of Abf2p with either acetyl-CoA or acetylphosphate did not result in the inhibition of its DNA-binding activity *in vitro* (Fig. S5).

Next, we tried to assess the effect of the succinylation of individual lysines on the DNA-binding activity of Abf2p. For the K162 identified by Weinert *et al.* (19), we generated two mutant versions. In the first version, K162 was substituted for arginine (Abf2-K162R), an amino acid that cannot be succinylated. The second version contained glutamate at this position (Abf2-K162E), which should mimic the succinylation of

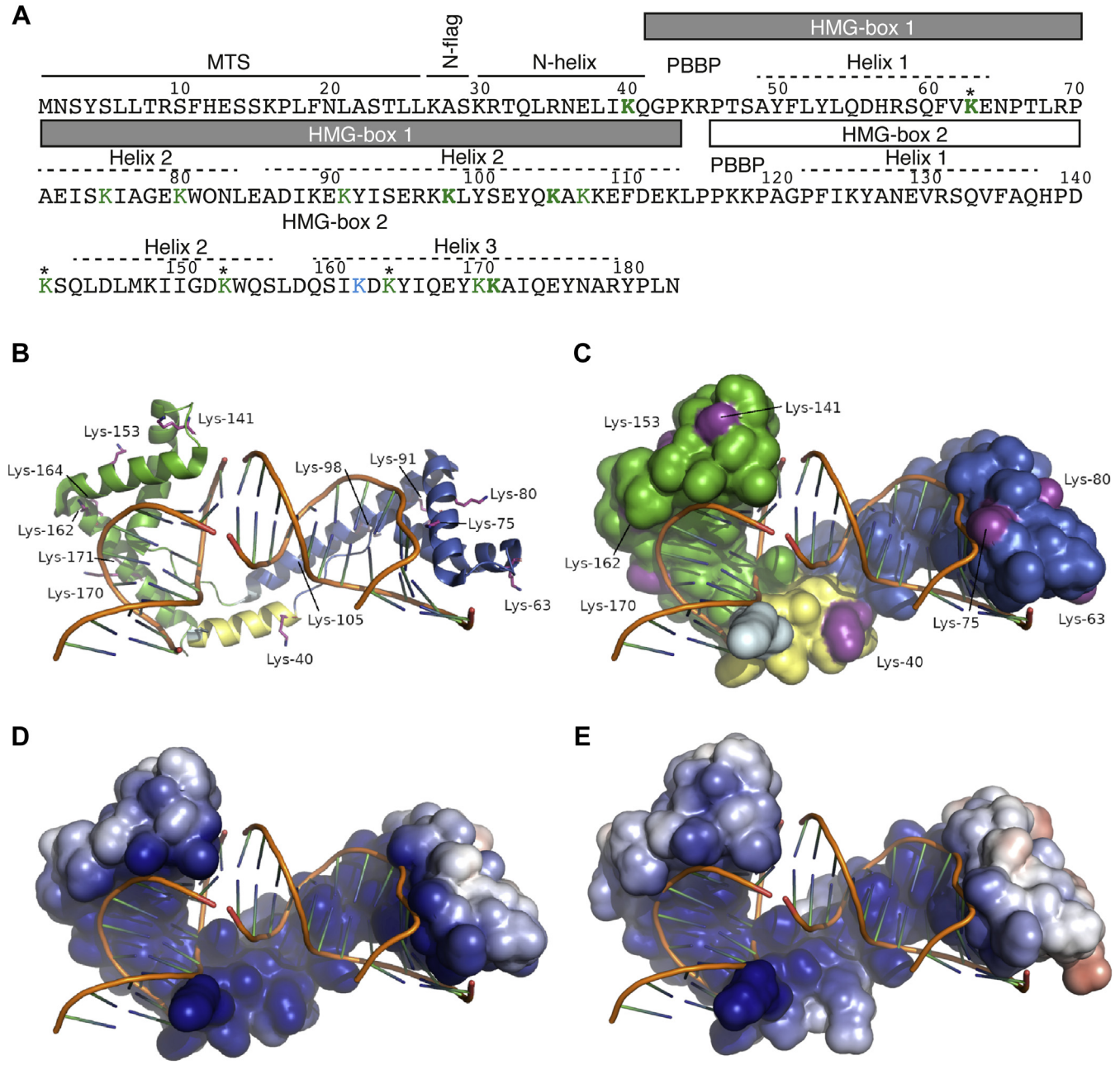

Figure 4. An overview of a single monomer bound to DNA from the Abf2p complex structure and a model of its succinylated form. *A*, sequence of Abf2p with highlighted structural regions based on the 3D structure of the protein (58). Lysines identified in a succinylated form *in vivo* in this study are in *green*. K162 identified by Weinert *et al.* (19) is in *blue*. The lysine residues having *in vitro* modified/unmodified ratios of more than 0.25 are in *bold* (*panel E*). MS analysis of Abf2p succinylated *in vitro* identified peptides containing Ksucc corresponding to all lysine residues except K27, K30, and K45. Lysine residues marked with *asterisks* (*) were also shown to be acetylated *in vivo* (46). *B*, an overview of half the Abf2p–DNA complex. The lysines found to be succinylated in this study are colored *magenta*, shown as *sticks*, and labeled. HMG box 1 is colored *blue*, HMG box 2 is *green*, the N-helix is *yellow*, and the N-flag is *light cyan*. This same coloring is used in the next panel. *C*, the same complex and the same view as before but showing the solvent-accessible surface area. Not all the succinylated lysines are visible. *D*, the solvent-accessible surface of Abf2p colored by electrostatic surface potential (the range is ±5 kT/e). *E*, the solvent-accessible surface of succinylated Abf2p colored by electrostatic surface potential (the same range as before). For the succinylated form, five residues were selected that had the greatest ratio of modified to unmodified forms *in vitro* and that were also found to be succinylated *in vivo*. B, basic amino acid; HMG box, high-mobility group box; MTS, mitochondrial targeting sequence.

this site. We found that the Abf2-K162E mutant exhibited different DNA-binding properties than the WT: at lower concentrations, its binding to the DNA probe was negligible, and at higher concentrations, it produced a smear (Fig. 5*C*). This indicates that the replacement of the positively charged lysine with the negatively charged glutamate (mimicking a negatively charged succinylated lysine) strongly affects the DNA-binding properties of the protein, which is consistent with our hypothesis that Abf2p succinylation greatly disfavors DNA-binding electrostatically. In contrast to Abf2-K162E, the Abf2-K162R mutant bound DNA similarly to the WT protein (Fig. 5*C*). However, when the Abf2-K162R protein was succinylated *in vitro*, the extent of its DNA-binding inhibition was similar to that of the WT (Fig. 5*D*), indicating that the

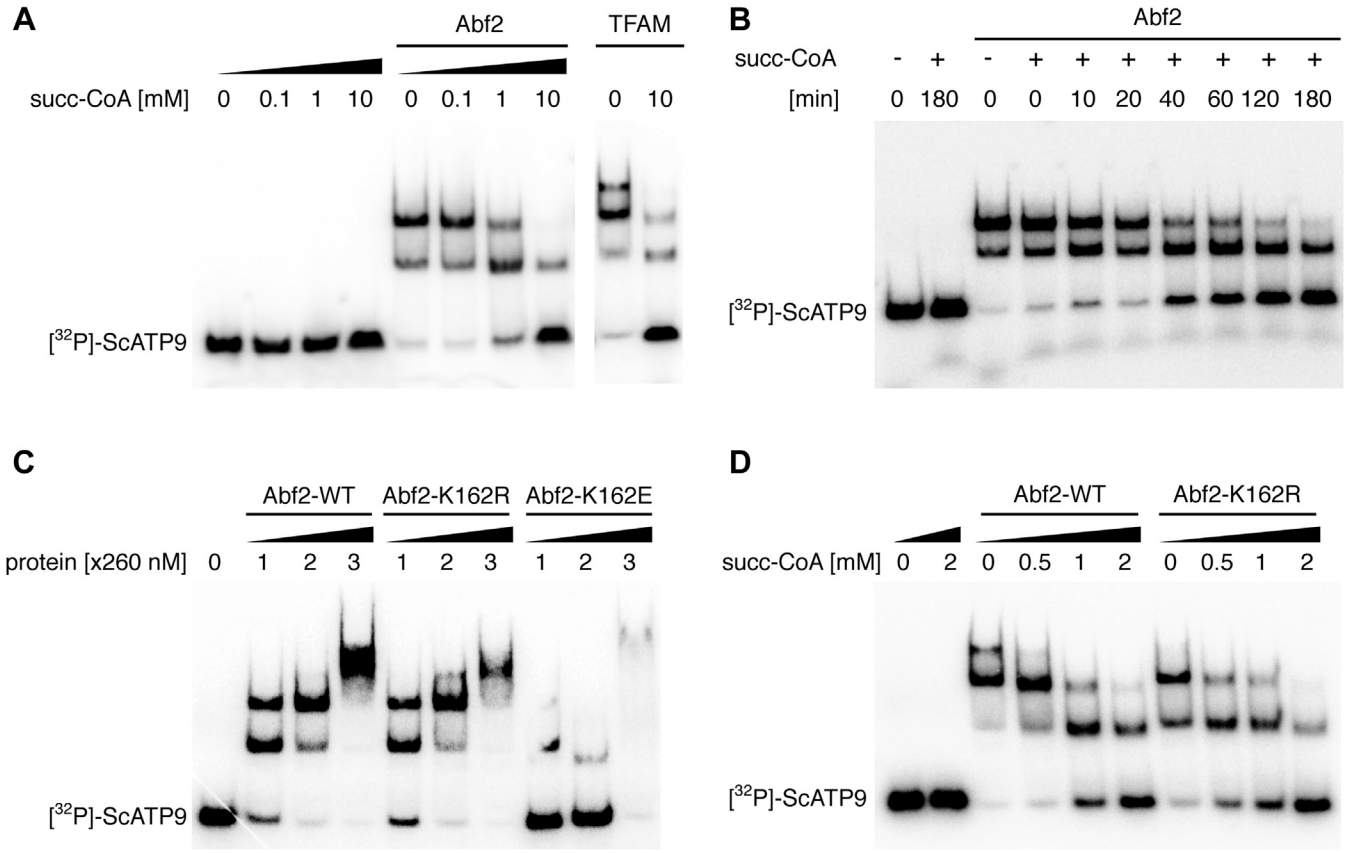

Figure 5. Succinylation of Abf2p *in vitro* inhibits its DNA-binding activity. *A*, succinylation of Abf2p and TFAM *in vitro* inhibits their DNA-binding activity in a concentration-dependent manner. Succinylation was performed at the indicated concentrations of succinyl-CoA (succ-CoA) for 3 h at 30 °C, and then, the DNA-binding activity was assessed by EMSA using radioactively labeled *ScATP9* as a probe. *B*, succinylation of Abf2p *in vitro* inhibits its DNA-binding activity in a time-dependent manner. Succinylation was performed in the presence of 10 mM succ-CoA at 30 °C for the indicated time periods. *C*, substitution of K162E affects binding of Abf2p to DNA *in vitro*. *D*, Abf2-K162R mutant protein is as sensitive to succinylation as the WT Abf2p.

observed decrease in DNA-binding is most likely caused by the succinylation of lysines in different positions within the protein. With the aim of identifying the combination of lysines whose succinylation accounts for the inhibition of Abf2p *in vitro*, we prepared a series of Abf2p mutants carrying multiple K-to-R substitutions. However, the introduction of these mutations into Abf2p invariably decreased its DNA-binding activity, making it difficult to distinguish between the inhibitory effect of succinylation and that of the K-to-R substitution(s) of the corresponding mutants (Fig. S6) (62).

To test whether the effect of succinylation on the DNA-binding activity *in vitro* is specific for *S. cerevisiae* Abf2p, or universal for mtHMG proteins, we purified recombinant versions of similar proteins from three additional yeast species, *Candida parapsilosis* (*Cp*Gcf1p) (63), *C. albicans* (*Ca*Gcf1p) (64), and *Yarrowia lipolytica* (*Yl*Mhb1p) (65). We observed that the effect of succinylation on their DNA-binding activities varied (Fig. S7). Whereas Abf2p and *Cp*Gcf1p were significantly inhibited by succinylation in the presence of 10 mM succinyl-CoA, the DNA binding of *Ca*Gcf1p and *Yl*Mhb1p was not substantially affected (Fig. S7). Furthermore, we found that *in vitro* succinylation of human mtHMG protein TFAM inhibits its DNA-binding activity to a similar degree as in case of Abf2p (Fig. 5*A*). Three lysine residues (K-95, K-190, and K-205) were found to be succinylated on TFAM in HeLa cells (19), indicating that lysine succinylation mediated by an increased level of succinyl-CoA may provide another link between metabolism and mt-nucleoid maintenance not only in *S. cerevisiae* but also in human cells. In contrast, regulation of TFAM *via* fumarate-mediated succination of a cysteine residue (66, 67) is not reflected by this means of regulation in case of Abf2p that lacks cysteines (Fig. 4*A*). All these data illustrate that regulation of mtHMG proteins by PTMs exhibits species-specific characteristics.

Based on the Abf2p–DNA complex shown in Figure 4, succinylation decreases the charge of the structure, with most of the effect occurring on the outer surface of the complex, where it could disrupt the formation of higher oligomers. It was previously demonstrated that Abf2p acts as a dimer (68). Because succinylation mostly affects lysines located on the surface of the molecule (Fig. 4), we tested whether it decreased the ability of Abf2p to form dimers. Using size-exclusion chromatography, we found that succinylated Abf2p did not lose the ability to dimerize (Fig. S8).

Succinylated Abf2p is resistant to degradation by ScLon protease in vitro

Previously, it was demonstrated that, when not bound to mtDNA, Abf2p is degraded by the ATP-dependent protease *Sc*Lon, which is another component of yeast mt-nucleoids (68).

We tested the effect of succinylation on the sensitivity of Abf2p to degradation by *Sc*Lon. We observed that Abf2p succinylated *in vitro* was more resistant to *Sc*Lon-mediated proteolysis than unmodified Abf2p (Fig. 6, *A* and *B*). Namely, the treatment of Abf2p with *Sc*Lon protease resulted in about 60% reduction of the amount of the protein (black bars in Fig. 6*B*), whereas succinylated Abf2p was mostly protected from degradation by the protease (white bars). Moreover, the addition of dsDNA, which protects unsuccinylated Abf2p from *Sc*Lon-mediated proteolysis, did not affect the susceptibility of the succinylated protein to degradation (Fig. 6, *A* and *B*). Because succinylated Abf2p is predominantly in a DNA-free form regardless of the presence of DNA, its resistance to proteolysis must be due to the succinylation. Moreover, the presence of dsDNA did not affect the protease activity of *Sc*Lon toward β-casein (Fig. 6*C*).

Discussion

Since its discovery in 2004 (18), lysine succinylation was found to affect a substantial part of the prokaryotic and eukaryotic proteomes. Because it is driven by the intracellular concentration of succinyl-CoA, it links metabolism to global changes in the PTMs of cellular proteomes, including those of cancer cells. The proteome of *S. cerevisiae* is not an exception, and many of its members were shown to be succinylated (19). The effects of succinylation were studied primarily on yeast histones, as this PTM provides another set of epigenetic marks regulating the chromatin state (69–71).

Mitochondria are the predominant sites of succinyl-CoA production, which arises from the decarboxylation of α-KG during the TCA cycle; it is therefore expected that mitochondrial proteins are highly prone to succinylation. However, a study of the yeast mitochondrial succinylome based on a proteomic analysis of purified mitochondria has been lacking. To observe the effects of protein succinylation on respiring mitochondria, we analyzed the succinylation state of proteins extracted from yeast mitoplasts that were prepared from cells grown on nonfermentable (glycerol + ethanol) carbon sources rather than on the fermentable (glucose or galactose) ones used by previous studies. As a result, we produced the first comprehensive list of *S. cerevisiae* mitochondrial proteins

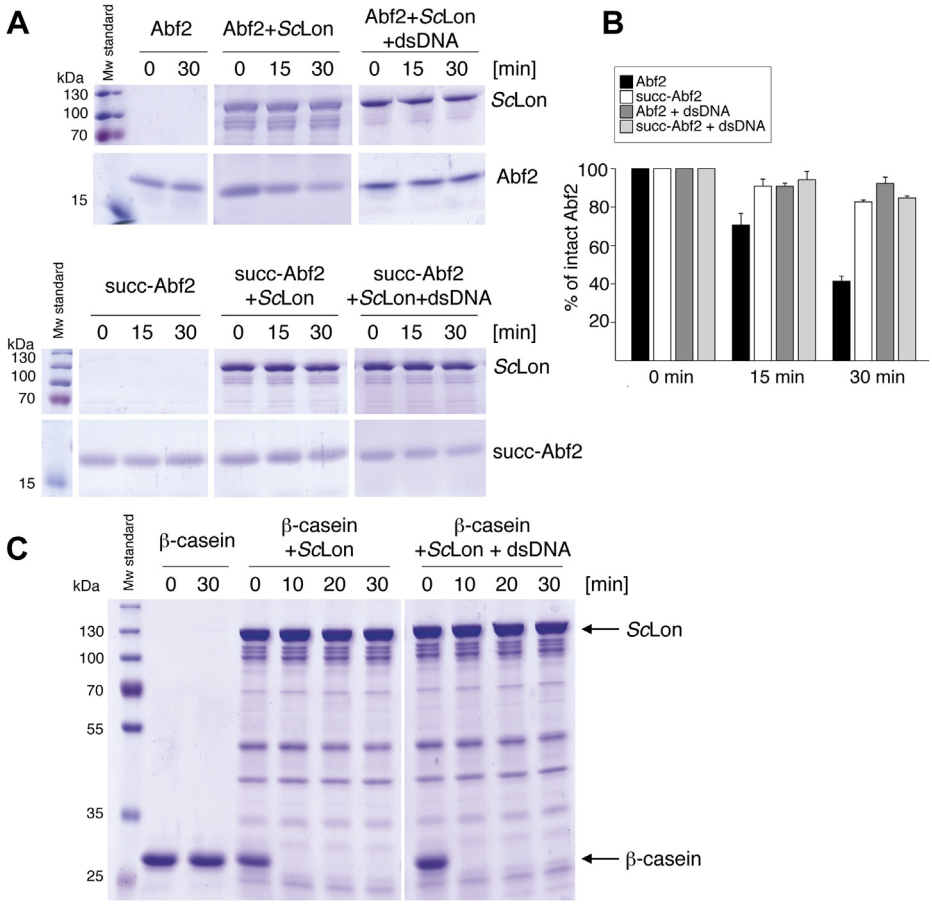

Figure 6. Succinylated Abf2p is less sensitive to digestion by the ATP-dependent *Sc*Lon protease. Nonsuccinylated (Abf2p) or *in vitro*–succinylated (succ-Abf2p) protein was incubated with purified *Sc*Lon in the presence or absence of a dsDNA probe. *A*, the course of an Abf2p *Sc*Lon-mediated digestion in reaction mixtures containing 2 mM ATP and 10 mM $MgCl_2$ on Coomassie Brilliant Blue–stained gels. The reactions were terminated at the indicated times and the samples loaded onto a 12% SDS-polyacrylamide gel. *B*, quantification of the digestion experiments shown in *panel A*. Band intensity evaluation of undigested Abf2p (Abf2 (%)) was performed with ImageJ (v.1.53) (104) separately for each studied protein. The height of a given bar represents the mean value, and the error bars show ± one SD from at least three separate measurements. *C*, the course of β-casein digestion by *Sc*Lon. β-casein was incubated with *Sc*Lon in the presence or absence of a dsDNA in a reaction mixture containing 2 mM ATP and 10 mM $MgCl_2$ for indicated times, and the proteins were separated on a 12% SDS-polyacrylamide gel.

modified by succinylation. We identified 314 mitochondrial proteins containing 1914 succinylated sites, 92.1% of which were not previously reported. From our data, it is not possible to assess the stoichiometry of succinylation even in the case of proteins containing a single Ksucc. Proteins with ≥2 Ksucc sites may constitute a heterogeneous population consisting of polypeptides carrying different combinations of Ksucc residues. As different patterns of succinylation (and PTMs including phosphorylation and other acylations) can result in a given protein having different biochemical properties, this may contribute to a significant increase in the complexity of the mitochondrial proteome.

Although we expanded the list of yeast succinylated mitochondrial proteins, it is likely that a substantial number of succinylation sites remain unidentified. This might be due in part to the low abundance of some proteins, whose succinylation may be below detection limit of our procedure. The succinylation pattern may also be influenced by the physiological conditions of the cell population, leading to different local concentrations of succinyl-CoA. Furthermore, the availability of potential acceptor lysine residues may differ because of their interactions with other intramitochondrial components (proteins, DNA, membrane), which may hinder their accessibility to succinyl-CoA. One possibility for increasing the overall level of succinylation is to boost the intracellular concentration of succinyl-CoA. To this end, we determined the mitochondrial succinylome of a *S. cerevisiae* strain lacking the α-subunit of the succinyl-CoA ligase Lsc1p. It was shown previously that a *lsc1*Δ mutant exhibits about a 3-fold higher level of succinylated proteins (19). Although succinylated proteins were indeed enriched in the mitoplast extract obtained from the *lsc1*Δ mutant, the list of succinylated proteins overlapped the WT mitochondrial succinylome to a large extent (Table S1). Combined with the fact that the increase in succinyl-CoA concentration in *lsc1*Δ is achieved by non-physiological means, we decided to focus on the dataset obtained from the WT cells.

Based on our analysis, succinylation occurs predominantly on lysine residues located in ordered and α-helical regions, whereas lysines within coiled regions are less likely to be affected. As expected for a nonenzymatic modification, lysines exposed to the surface are slightly more prone to succinylation (47). Indeed, when we mapped the succinylated lysines on the 3D structure of Abf2p, all of them (with the possible exception of K162) were found on the outer surface of the protein (Fig. 4, *B–E*, see also below). This illustrates that it is physical proximity rather than a specific amino acid sequence motif that makes particular lysines susceptible to succinylation, which supports ongoing efforts to develop succinylation prediction algorithms based on secondary structures and evolutionary information rather than on simply trying to identify sequence motifs (72).

Because the majority of the components of the mt-nucleoid were succinylated, it is likely that this PTM plays a role in their metabolism. To investigate the possible functional importance of succinylation in the regulation of the mt-nucleoid, we analyzed the effect of succinylation on the DNA-binding activity of Abf2p, known to mediate the bending and compacting of mtDNA in *S. cerevisiae* (reviewed in (54)). Of the twenty-five lysine residues present in the mature form of Abf2p (lacking the MTS) (Fig. 4*A*), thirteen were succinylated *in vivo*. This prompted us to investigate the effect of succinylation on the DNA-binding activity of Abf2p *in vitro*. We found that incubation of Abf2p with succinyl-CoA, but not with acetyl-CoA or acetylphosphate, inhibited its binding to the DNA probe in EMSA experiments (Figs. 5, *A* and *B* and S5) and that this inhibition is due to the modification of the protein and not to the presence of succinyl-CoA in the reaction mixture (Fig. S4). MS analysis revealed that all the succinylated lysines identified by analyzing immunoprecipitated Abf2p are also modified *in vitro* (Fig. 4*A*). To assess whether there are any specific lysine residues whose succinylation affects DNA-binding properties of Abf2p, we tested several mutant versions carrying lysine to arginine substitutions, which cannot be succinylated. Almost all of these mutants exhibited decreased DNA-binding activity *in vitro*, even without succinyl-CoA treatment (62). This excluded the possibility of investigating the effect of succinylation on individual lysine residues on the ability of Abf2p to compact mt-nucleoids *in vivo*, as it would be impossible to distinguish between the phenotypic effects of the K-to-R substitutions themselves from the effects arising from their lack of succinylation. On the other hand, the substitution of a single lysine (K162) with glutamate (mimicking the negative charge of Ksucc) in the Abf2-K162E mutant greatly affected its DNA-binding activity (Fig. 5*C*). This indicates that the succinylation of only one or a very few lysines can have a profound effect on binding of Abf2p to mtDNA.

In vitro succinylated Abf2p not only exhibits decreased DNA-binding activity but also is more resistant to the *Sc*Lon protease (Fig. 6). It has been shown that the initial cleavage sites of human Lon protease are preferentially between hydrophobic amino acids located within highly charged environments on the surface of the folded protein (73). Assuming that *Sc*Lon cleaves its substrates in a similar manner, succinyl groups on lysines found predominantly on the surface of the Abf2p dimer might prevent *Sc*Lon from recognizing its characteristic surface sites and thus inhibit the initiation of proteolysis.

The mature form of Abf2p is a relatively basic protein (predicted pI = 9.68) containing in total 33 lysines plus arginines. Lysines are the prevalent (78.8%) basic residues in its HMG boxes. This bias toward lysines is not a common feature of all basic DNA-binding proteins, however. For example, *S. cerevisiae* histones Hho1p (H1), Htb1p (H2B), and Htb2p (H2B) exhibit this bias, but in Hht1p (H3), Hht2p (H3), Hta1p (H2A), and Hta2p (H2A), the lysine-to-arginine ratio is approximately 1. Similarly, there is no bias toward lysines in *E. coli* nucleoid–associated proteins HU, IHF, H-NS, or FIS, yet lysines constitute still at least 7% of total amino acid residues of these DNA-binding proteins. Perhaps, lysine-rich DNA-binding proteins are more susceptible to modifications such as succinylation, which may affect their DNA binding and interactions with other proteins. Because a substantial fraction of lysines is located on the surface of Abf2p, the addition of a

succinyl group to a lysine residue would change the Abf2p surface, thereby potentially affecting its interactions with other mt-nucleoid proteins.

Because the *in vitro* succinylation of mtHMG proteins from four different yeast species has different effects on their DNA-binding activity (Fig. S7), this PTM is not universally adopted as a means of regulating their activity. Even mtHMG proteins from relatively closely related species (*Ca*Gcf1 and *Cp*Gcf1) differ in the effect that succinylation has on their DNA-binding ability. Furthermore, the lysines identified as succinylated on Abf2p *in vivo* are not conserved in species closely related to *S. cerevisiae* (see Fig. S1 in (54)). Although it is impossible to generalize based on this single example, it is conceivable that this kind of species-specific regulation of a protein by succinylation might be more common.

An increase in the activity of the TCA cycle results in changes in the concentration of its intermediates, including succinyl-CoA. For example, in *E. coli*, the concentrations of succinyl-CoA range from 0.233 mM, when cells are grown on glucose, to 1.44 mM, when cells are grown on glycerol (74). *S. cerevisiae* is a Crabtree-positive yeast species that when grown on glucose, first ferments the sugar to ethanol and then, after a short metabolic adaptation called diauxic shift, enters a respiratory phase of growth. This transition is accompanied by several changes in mitochondrial function and structure and reflected by reorganization of mitochondrial metabolism including the activation of the TCA cycle (75). When we inspected mt-nucleoids in cells taken from fermentative, diauxic shift and respiratory phases of the growth, we observed dramatic changes in both their number per cell and their appearance (Fig. S9). Of note, the subunits of α-KG dehydrogenase (Kgd1p and Kgd2p), the principal enzymes of the TCA cycle, were shown to be components of the *S. cerevisiae* mt-nucleoid (53, 57, 76), and thus, succinyl-CoA could be generated in its close proximity, thereby promoting succinylation of the mt-nucleoid-associated proteins. In fact, it was shown that α-KG dehydrogenase may act as a catalyst of the succinylation reaction (71, 77), so it may directly facilitate the modification of those proteins in its vicinity, thus affecting their biochemical properties. In the case of Abf2p, succinylation would decrease its ability to bind mtDNA and thus promote changes in mt-nucleoids observed during the diauxic shift. Of note, succinylation of several nucleoid-associated proteins was suggested to affect their DNA binding, structural integrity, or interaction with other proteins in *E. coli* (55), indicating that this model might be also relevant for the maintenance of the bacterial chromosome. Alternatively (or in parallel), succinylation of components of the respiratory complexes and/or the ATP synthase might result in their altered activity that could counterbalance the overactive TCA cycle during the respiratory growth phase. Future comparative studies aimed at careful quantification of succinylome of cells under defined metabolic states will shed more light on the functional significance of this PTM for linking metabolism and other mitochondrial (or cellular) functions.

By providing a comprehensive list of succinylated *S. cerevisiae* mitochondrial proteins and functional analysis of one of its putative targets, our study represents a primer for the systematic investigation of the functional importance of succinylation in mitochondria-related activities.

Experimental procedures

Microbial strains

S. cerevisiae strain SCY325 (*MAT*α, *ade2-1 his3-11,15 leu2-3112 trp1-1 ura3-1 can1*) (78) and its *lsc1*Δ derivative (*MAT*α, *ade2-1 his3-11,15 leu2-3112 trp1-1 ura3-1 can1 lsc1*Δ*::LEU2*) were used for the purification of mitoplasts. An *lsc1*Δ strain lacking the entire ORF for the α-subunit of succinyl-CoA ligase Lsc1p was derived from the SCY325 strain by one-step recombinational deletion using an *LEU2* cassette. The deletion cassette was amplified from the genomic DNA of *S. cerevisiae* strain GG595 (*MAT*α/*MAT*a *HO/HO ura3/ura3* (provided by H. Yde Steensma, Leiden University, The Netherlands)) by PCR using the LSC1_DC_LEU2_F and LSC1_DC_LEU2_R primers (Table S4) and Phusion Hot Start II DNA Polymerase (Thermo Fisher Scientific). Yeast cells were transformed using the LiAc/PEG/ssDNA method (79, 80), selected based on leucine prototrophy, and the cassette insertion was verified by colony PCR using the pLSC1_5_F and pLEU2_5_R (5′ region) and pLEU2_3_F and pLSC1_3_R (3′ region) primers (Table S4). The *ScATP9* probe was amplified using a DNA template prepared from the *S. cerevisiae* strain W303-1A (*MATa, leu2-3112 trp1-1 can1-100 ura3-1 ade2-1 his3-11,15*), which was from the collection of the Departments of Genetics and Biochemistry, Comenius University in Bratislava. For *Sc*Lon purification, the strain pSEY c68-ScLON expressing the WT *Sc*Lon gene from the *GAL1* promoter of the centromere-based plasmid pSEYc68 was used (81). *E. coli* strains BL21 Star (F^-, *ompT*, *hsdS*, r^-m^-, *gal*, *dcm*, *rne131*(*DE3*)), Rosetta 2 (DE3) (F^-, *ompT*, $hsdS_B$, $r_B^-m^-$, *gal*, *dcm* (DE3), *pRARE2* (Cam^R)), and DH5α (F^-, *φ80dlacZΔM15, Δ(lacZYA-argF) U169 deoR, recA1, endA1, hsdR17* (rk^-, mk^+), *λ, thi-1, gyrA96, relA1, glnV44, nupG*) were purchased from Life Technologies.

Mitoplast preparation

S. cerevisiae strain SCY325 was cultivated in YPGE medium (yeast extract (1% (w/v)), Bacto Peptone (2% (w/v)), glycerol (3% (v/v)), ethanol (2% (v/v))). Mitochondria were isolated as described (82). Mitoplasts were prepared by the addition of 20 mM Hepes-KOH (pH 7.4) in a 10:1 volume ratio to the mitochondrial pellet. The suspension was incubated on ice for 30 min, centrifuged at 12,000*g* at 4 °C, and washed twice with ice-cold 0.6 M sorbitol buffer with 20 mM Hepes-KOH (pH 7.4). Freshly prepared mitoplasts were stored at −80 °C for further use.

For diauxic shift experiment, the cells of the *S. cerevisiae* strain SCY325 were inoculated at density of A_{600} = 0.2 into YPD medium (yeast extract (1% (w/v)), Bacto Peptone (2% (w/v)), glucose (2% (w/v))). The growth was monitored by measuring A_{600}, and simultaneously, the glucose levels were determined as described (83).

Peptide preparation for Ksucc enrichment and MS analysis

Six milligrams of mitoplasts per WT and *lsc1*Δ biological triplicates were freeze-thawed; proteins were precipitated with 5 volumes of −20 °C acetone and sedimented (16,100*g*, 30 min, 4 °C). Pellets were washed 3 times and air-dried. Proteins were dissolved in 6.4 M urea, reduced with 5 mM DTT, and alkylated with 40 mM chloroacetamide. After dilution in 3 volumes of triethylammonium bicarbonate buffer, pH 8.0 (50 mM final concentration), the proteins were trypsin-digested (1:20 w/w) overnight. The acidified (with 0.5% (v/v) TFA) and oxidized (with 100 mM hydrogen peroxide) peptide solution was clarified by centrifugation and purified on a reversed-phase column (Supelclean LC-18 SPE; pre-washed with acetonitrile (ACN) followed by 0.1% (v/v) TFA). TFA-washed peptides (0.1%) were eluted from the matrix with TA70 (70% (v/v) ACN, 0.03% (v/v) TFA). After pH adjustment using Tris-HCl, pH 8, the eluate was divided, so that 5% of the sample could be used for the MS analysis of the protein background and 95% for Ksucc enrichment. The peptide aliquots were vacuum dried.

Enrichment of Ksucc-containing peptides for MS analysis

Peptides were dissolved in the IP buffer (100 mM NaCl, 1 mM EDTA, 20 mM Tris-HCl, pH 8.0, 0.5% (v/v) NP-40) with cOmplete Protease Inhibitor Cocktail (Roche), and the suspension was cleared by centrifugation. Peptides were incubated overnight at 6 °C with 30 µl of drained and PBS-washed Pan anti-succinyllysine antibody agarose conjugated resin (PTM Biolabs). The resin-bound peptides were washed using the IP buffer with and without 0.5% (v/v) NP-40 and using 50 mM ammonium bicarbonate. Succinylated peptides were eluted with 0.1% (v/v) TFA and vacuum-dried.

MS analyses

Peptide samples in biological triplicates, from both total WT and *lsc1*Δ mitoplast protein digests and their corresponding Ksucc enrichments, were dissolved in 0.1% (v/v) TFA and 2% (v/v) ACN. The samples were loaded onto a trap column (PepMap100 C18, 300 µm × 5 mm, Dionex) and separated with a C18 column (Acclaim PepMap C18, 75 µm × 500 mm, Dionex) on an UltiMate 3000 RSLCnano system (Dionex) in a 120-min gradient (3–43% B), curve 7, and a flow rate of 300 nl/min. The two mobile phases used were (A) 0.1% (v/v) formic acid and (B) 80% (v/v) ACN with 0.1% (v/v) formic acid. Eluted peptides were sprayed directly into an Orbitrap Elite mass spectrometer (Thermo Scientific), and spectral datasets were collected in a data-dependent mode using the Top15 strategy to select precursor ions for higher-energy collisional dissociation fragmentation (84). Each of the samples was analyzed in three technical replicates. The resulting datasets were processed by MaxQuant, version 1.5.3.30 (85), using the built-in Andromeda search engine with carbamidomethylation (C) and oxidation (M) set as permanent modifications. For the protein background, unmodified lysine and protein N-terminal acetylation were set as variable modifications permitting 2 missed tryptic cleavages. The variable search parameters for the Ksucc-enriched samples were lysine succinylation and protein N-terminal acetylation permitting four missed tryptic cleavages. The search was performed against a *S. cerevisiae* protein database downloaded on May 25, 2019, from https://www.uniprot.org/ containing 6049 entries. Identified protein groups, succinylation sites, and a summary of the analysis are in Table S1.

Data analyses

Only MS/MS-identified protein groups belonging to the high-confidence mitochondrial proteomes from Di Bartolomeo *et al.* (75), Morgenstern *et al.* (86), and Vögtle *et al.* (87) were considered. The same datasets were also used to annotate the localization of succinylated proteins by Weinert *et al.* (19) and acetylated proteins by Henriksen *et al.* (46) for comparative analysis. GOs were analyzed using either the PANTHER Overrepresentation Test tool (binomial test) (88) or YeastMine GO enrichment (Holm-Bonferroni correction) (89). The mitochondrial proteins detected in this study served as the reference. The medians for protein-per-cell abundances are from (56). Systematic gene name annotations and amino acid sequences were taken from the *Saccharomyces* Genome Database (90). The *Saccharomyces* Genome Database list of "mt-nucleoid" cellular component genes (GO:0042645) was also used. The sequence logos of the regions adjacent to succinylated lysine sites (the sequence windows were imported from MaxQuant) were analyzed using WebLogo 3.7.4 (91) and Seq2Logo 2.0 (92). Protein structural features were predicted using the MMseqs method of NetSurfP-2.0 (48). The differences between the predicted values of the properties of succinylated and nonsuccinylated lysines within succinylated proteins were evaluated using two-tailed t-tests with unequal variances (Microsoft Excel). MTSs were predicted by TargetP-2.0 (50).

DNA manipulations

Oligonucleotides (Table S4) were synthesized by Microsynth AG. The plasmids pGEX-6P-2-ScABF2noMP, pGEX-6P-2-YlMHB1noMP, and pGEX-6P-2-CpGCF1noMP are described in (65, 93), and the plasmid pGEX-6P-2-CaGCF1noMP in (64). Plasmid expression vectors carrying substitutions within the *ABF2* sequence were constructed by inverse PCR using the corresponding pairs of 5′-end phosphorylated primers and pGEX-6P-2-ScABF2noMP (for Abf2_K162R, Abf2_K162E, and Abf2_K117,118R), pGEX-6P-2-ScABF2noMP-K117,118R (for Abf2_K44,117,118R), and pGEX-6P-2-ScABF2noMP-K162R (for Abf2_4K-4R) as templates (Table S4). After amplification by Phusion HF DNA polymerase (Thermo Scientific), the PCR fragments were ligated by T4 DNA ligase (Thermo Scientific) and transformed into *E. coli* DH5α, and the plasmids were isolated using the plasmid QIAprep Spin Miniprep kit from Qiagen. The sequence of each construct was verified by Sanger DNA sequencing in Microsynth AG.

Effect of succinylation on the DNA-binding activity of yeast mtHMG proteins assessed by EMSA

Recombinant Abf2p, its mutant variants, other yeast mtHMG proteins, and human TFAM used for DNA-binding assays were purified from extracts from *E. coli* BL21 Star (DE3) cells transformed with the corresponding plasmid construct as described (68, 93). Protein concentration was determined using the Bradford assay (94), and the purity was assessed by 12% SDS-PAGE (95). The 50-bp-long DNA substrate derived from the *S. cerevisiae atp9* gene was amplified by PCR from the genomic DNA of *S. cerevisiae* strain W303-1A using the DreamTaq DNA polymerase (Thermo Scientific) and primers *Sc*ATP9_15_D and *Sc*ATP9_50_R (Table S4); the resulting dsDNA was 5′ end-labeled using T4 polynucleotide kinase (Thermo Scientific) and [γ^{32}P]ATP (3000 Ci/mmol). EMSA experiments using 260 nM of the tested DNA-binding proteins (unless stated otherwise) were performed as described (93). Succinylation *in vitro* was performed at 30 °C in the presence of the indicated concentrations of succinyl-CoA (Sigma-Aldrich).

Expression and purification of ScLon

For *Sc*Lon isolation and purification, the *S. cerevisiae* Δ*lon* strain carrying the plasmid pSEY c68-*Sc*LON (81) was grown to the early stationary phase in yeast synthetic medium (0.67% (w/v) yeast nitrogen base with ammonium sulfate) supplemented with 0.2% (w/v) glucose, 1.5% (w/v) galactose, 0.5% (w/v) casamino acids (Difco), 0.002% (w/v) adenine, and 0.002% (w/v) tryptophan. Mitochondria were isolated and purified as described (82) and *Sc*Lon carrying a C-terminal 6× His tag was purified as described previously (81). In brief, mitochondria corresponding to 10 mg/ml of proteins were resuspended in buffer A (20 mM Hepes-KOH, pH 8.0, 150 mM NaCl, 5 mM $MgCl_2$, 20% (v/v) glycerol) containing 1 mM ATP and 1.6 mg of Lubrol/mg of mitochondrial protein. The lysate was centrifuged at 200,000*g* at 4 °C for 10 min, and the supernatant was applied to a Ni-NTA Agarose resin (Qiagen). The column was washed with five column volumes of buffer A containing 40 mM imidazole, and bound protein was then stepwise eluted with buffer A containing 0.1, 0.2, and 0.3 M imidazole. The enzymatic activity of the purified *Sc*Lon was then determined by β-casein degradation as described (68).

ScLon proteolytic assay

For proteolytic assays, recombinant *S. cerevisiae* Abf2p lacking the MTS (first 26 amino acid residues) and carrying an N-terminal His tag (6× His-GST) (96) was purified from *E. coli* Rosetta 2 (DE3) as described previously (68). In brief, the cells were resuspended in buffer B (50 mM ammonium acetate, pH 7.3, 1 M KCl, 10% (v/v) glycerol) with the addition of 0.1% (v/v) Tween 20 and 0.2 mg/ml lysozyme followed by a short incubation at room temperature (RT) and sonication on ice. The cell lysate was centrifuged (30,000*g*, 30 min, 6 °C), and the supernatant was loaded onto a Ni-Sepharose 6 Fast Flow column (GE Healthcare). The eluted protein was incubated overnight with PreScission protease (GE Healthcare) according to the manufacturer's instructions and then applied to a Glutathione Sepharose 4 Fast Flow column (GE Healthcare). Abf2p was eluted in the unbound fraction, diluted (2.5×) with buffer B (without KCl), and loaded onto a Heparin Sepharose 6 Fast Flow column (GE Healthcare). The bound protein was eluted with a stepwise KCl gradient, concentrated, and purified on a Superdex 75 10/300GL column (GE Healthcare). Succinylated Abf2p for proteolytic assays was prepared by incubating purified Abf2p with 10 mM succinyl-CoA in 20 mM Tris HCl (pH 7.4), 50 mM NaCl, and 1 mM EDTA for 2 h at RT. Free succinyl-CoA was removed by gel filtration on a Superdex 75 10/300GL column (GE Healthcare) equilibrated with buffer C (50 mM ammonium acetate (pH 7.3), 500 mM KCl, 5% (v/v) glycerol). The given amounts of substrate proteins (Abf2p, succinylated Abf2p, casein) were incubated in an *Sc*Lon reaction buffer (50 mM Tris HCl, pH 8.5, 10 mM $MgCl_2$, 2 mM ATP). A 750-bp DNA fragment (*Kpn*I/*Hin*dIII) from the pOPINM-XRCC6BP1 plasmid construct (4 μM) was used as the dsDNA probe. Each reaction was carried out at 30 °C for 30 min with aliquots withdrawn at the indicated times. Reaction products were analyzed by SDS-PAGE in 12% polyacrylamide gels and Coomassie Brilliant Blue R250 staining.

Succinylated Abf2p modeling

The model of succinylated Abf2p was built by manually combining the coordinates of the succinyl moiety of Ksucc from a succinylated histone 3 peptide in complex with sirtuin-5 (PDB ID: 3RIY) (97) with the side chains of those lysines from the previously reported 2.18 Å Abf2p structure (PDB ID: 5JH0) (58) that were found to be succinylated in our IP assays. After torsion angle adjustments to remove steric clashes introduced by these modifications, this structure's geometry was regularized by Refmac5 (98) using a geometry database derived from the Ksucc of 3RIY. The resulting structure was then minimized against the AMBER 14 forcefield (99) in Chimera (100). The geometry of the resulting structure was checked using MolProbity (101) and was found to be sufficient for the purposes of this study. The electrostatic surface of both succinylated and nonsuccinylated Abf2p was calculated using PDB2PQR and APBS (102). Coordinate manipulation and structure visualization were done using the PyMOL Molecular Graphics System, version 2.3.0, Schrödinger, LLC.

Data availability

The MS proteomics data have been deposited in the ProteomeXchange Consortium *via* the PRIDE (103) partner repository with the dataset identifier PXD023604 (username: reviewer_pxd023604@ebi.ac.uk; password: zMPT8wo0).

Supporting information—This article contains supporting information (19, 46, 56, 75, 83, 86, 87, 91, 92, 105).

Acknowledgments—We thank Filip Tomáška for quantitative analysis of mitochondrial nucleoids and Dr Martin Valachovič (Institute of Animal Biochemistry and Genetics, Centre of Biosciences, Slovak

Academy of Sciences, Bratislava, Slovakia) and Dr H. Yde Steensma (Leiden University, The Netherlands) for kindly providing the *S. cerevisiae* strains SCY325 and GG595, respectively.
This study was supported by the Operation Program of Integrated Infrastructure for the project Advancing University Capacity and Competence in Research, Development and Innovation, ITMS2014+: 313021X329, cofinanced by the European Regional Development Fund and with the support of the Operational Program Integrated Infrastructure for the project Center for Biomedical Research–BIOMEDIRES II stage, ITMS: 313011W428, and with the support of the Interreg V-A Slovakia-Austria program (www.sk-at.eu) for the project StruBioMol, ITMS: 305011X666 and cofinanced by the European Regional Development Fund. CIISB, Instruct-CZ Centre of Instruct-ERIC EU consortium, funded by MEYS CR infrastructure project LM2018127, is gratefully acknowledged for the financial support of the measurements at the CEITEC Proteomics Core Facility.

Author contributions—J. F. and L. T. conceptualization; J. F., B. K., J. B., N. K., N. C., K. H., J. A. B., G. O., V. L., K. P., P. B., and L. T. investigation; J. F., N. K., N. C., J. A. B., K. P., and L. T. visualization; J. F., B. K., J. B., N. K., K. H., J. A. B., V. P., P. B., and L. T. methodology; J. F., B. K., N. K., and L. T. writing–original draft; J. F., B. K., J. B., N. K., N. C., K. H., J. A. B., G. O., V. L., B. S., V. P., K. P., J. N., P. B., E. K., and L. T. writing–review and editing; J. B., V. L., B. S., and Z. Z. formal analysis; Z. Z., V. P., J. N., P. B., E. K., and L. T. resources; Z. Z., V. P., J. N., P. B., E. K., and L. T. funding acquisition; V. P., P. B., E. K., and L. T. supervision; V. P., P. B., E. K., and L. T. project administration.

Funding and additional information—Funding was provided by the Slovak Research and Development Agency (APVV) (APVV-15-0022 and APVV-19-0068 [to L. T.], APVV-18-0239 [to J. N.], APVV-15-0375 and APVV-19-0298 [to E. K.]) and the Scientific Grant Agency of the Ministry of Education, Science, Research and Sport of the Slovak Republic (VEGA) (1/0061/20 [to L. T.], 1/0027/19 [to J. N.], 2/0075/18 [to E. K.]).

Conflict of interest—The authors declare that they have no conflicts of interest with the contents of this article.

Abbreviations—The abbreviations used are: ACN, acetonitrile; α-KG, α-ketoglutarate; 2HG, 2-hydroxyglutarate; GO, gene ontology; HMG box, high-mobility group box; IP, immunoprecipitation; Ksucc, 6-*N*-succinyl-l-lysine; mtDNA, mitochondrial DNA; mtHMG protein, mitochondrial high-mobility group box containing protein; mt-nucleoid, mitochondrial nucleoid; MTS, mitochondrial targeting sequence; non-Ksucc, nonsuccinylated lysines; PTM, post-translational modification; TCA, tricarboxylic acid.

References

1. Cagin, U., and Enriquez, J. A. (2015) The complex crosstalk between mitochondria and the nucleus: What goes in between? *Int. J. Biochem. Cell Biol.* **63**, 10–15
2. Guaragnella, N., Coyne, L. P., Chen, X. J., and Giannattasio, S. (2018) Mitochondria-cytosol-nucleus crosstalk: Learning from *Saccharomyces cerevisiae*. *FEMS Yeast Res.* **18**, foy088
3. Pfanner, N., Warscheid, B., and Wiedemann, N. (2019) Mitochondrial proteins: From biogenesis to functional networks. *Nat. Rev. Mol. Cell Biol.* **20**, 267–284
4. Graves, J. D., and Krebs, E. G. (1999) Protein phosphorylation and signal transduction. *Pharmacol. Ther.* **82**, 111–121
5. Tomáška, Ľ. (2000) Mitochondrial protein phosphorylation: Lessons from yeasts. *Gene* **255**, 59–64
6. Rao, S., Gerbeth, C., Harbauer, A., Mikropoulou, D., Meisinger, C., and Schmidt, O. (2011) Signaling at the gate: Phosphorylation of the mitochondrial protein import machinery. *Cell Cycle* **10**, 2083–2090
7. Frankovsky, J., Vozáriková, V., Nosek, J., and Tomáška, Ľ. (2021) Mitochondrial protein phosphorylation in yeast revisited. *Mitochondrion* **57**, 148–162
8. Guo, X., Niemi, N. M., Coon, J. J., and Pagliarini, D. J. (2017) Integrative proteomics and biochemical analyses define Ptc6p as the *Saccharomyces cerevisiae* pyruvate dehydrogenase phosphatase. *J. Biol. Chem.* **292**, 11751–11759
9. Guo, X., Niemi, N. M., Hutchins, P. D., Condon, S. G. F., Jochem, A., Ulbrich, A., Higbee, A. J., Russell, J. D., Senes, A., Coon, J. J., and Pagliarini, D. J. (2017) Ptc7p dephosphorylates select mitochondrial proteins to enhance metabolic function. *Cell Rep.* **18**, 307–313
10. Reinders, J., Wagner, K., Zahedit, R. P., Stojanovski, D., Eyrich, B., van der Laan, M., Rehling, P., Sickman, A., Pfanner, N., and Meisinger, C. (2007) Profiling phosphoproteins of yeast mitochondria reveals a role of phosphorylation in assembly of the ATP synthase. *Mol. Cell. Proteomics* **6**, 1896–1906
11. Renvoisé, M., Bonhomme, L., Davanture, M., Valot, B., Zivy, M., and Lemaire, C. (2014) Quantitative variations of the mitochondrial proteome and phosphoproteome during fermentative and respiratory growth in *Saccharomyces cerevisiae*. *J. Proteomics* **106**, 140–150
12. Schmidt, O., Harbauer, A. B., Rao, S., Eyrich, B., Zahedi, R. P., Stojanovski, D., Schönfisch, B., Guiard, B., Sickmann, A., Pfanner, N., and Meisinger, C. (2011) Regulation of mitochondrial protein import by cytosolic kinases. *Cell* **144**, 227–239
13. Ringel, A. E., Tucker, S. A., and Haigis, M. C. (2018) Chemical and physiological features of mitochondrial acylation. *Mol. Cell.* **72**, 610–624
14. Garland, P. B., Shepherd, D., and Yates, D. W. (1965) Steady-state concentrations of coenzyme A, acetyl-coenzyme A and long-chain fatty acyl-coenzyme A in rat-liver mitochondria oxidizing palmitate. *Biochem. J.* **97**, 587–594
15. Hansford, R. G., and Johnson, R. N. (1975) The steady state concentrations of coenzyme A-SH and coenzyme A thioester, citrate, and isocitrate during tricarboxylate cycle oxidations in rabbit heart mitochondria. *J. Biol. Chem.* **250**, 8361–8375
16. Ghanta, S., Grossmann, R. E., and Brenner, C. (2013) Mitochondrial protein acetylation as a cell-intrinsic, evolutionary driver of fat storage: Chemical and metabolic logic of acetyl-lysine modifications. *Crit. Rev. Biochem. Mol. Biol.* **48**, 561–574
17. Wagner, G. R., Bhatt, D. P., O'Connell, T. M., Thompson, J. W., Dubois, L. G., Backos, D. S., Yang, H., Mitchell, G. A., Ilkayeva, O. R., Stevens, R. D., Grimsrud, P. A., and Hirschey, M. D. (2017) A class of reactive acyl-CoA species reveals the non-enzymatic origins of protein acylation. *Cell Metab* **25**, 823–837
18. Rosen, R., Becher, D., Büttner, K., Biran, D., Hecker, M., and Ron, E. Z. (2004) Probing the active site of homoserine trans-succinylase. *FEBS Lett.* **577**, 386–392
19. Weinert, B. T., Schölz, C., Wagner, S. A., Iesmantavicius, V., Su, D., Daniel, J. A., and Choudhary, C. (2013) Lysine succinylation is a frequently occurring modification in prokaryotes and eukaryotes and extensively overlaps with acetylation. *Cell Rep.* **4**, 842–851
20. Zhang, Z., Tan, M., Xie, Z., Dai, L., Chen, Y., and Zhao, Y. (2011) Identification of lysine succinylation as a new post-translational modification. *Nat. Chem. Biol.* **7**, 58–63
21. Waitkus, M. S., Diplas, B. H., and Yan, H. (2018) Biological role and therapeutic potential of IDH mutations in cancer. *Cancer Cell* **34**, 186–195
22. Dang, L., and Su, S.-S. M. (2017) Isocitrate dehydrogenase mutation and (R)-2-hydroxyglutarate: From basic discovery to therapeutics development. *Annu. Rev. Biochem.* **86**, 305–331
23. Li, F., He, X., Ye, D., Lin, Y., Yu, H., Yao, C., Huang, L., Zhang, J., Wang, F., Xu, S., Wu, X., Liu, L., Yang, C., Shi, J., He, X., *et al.* (2015) $NADP^+$-IDH mutations promote hypersuccinylation that impairs mitochondria respiration and induces apoptosis resistance. *Mol. Cell.* **60**, 661–675

24. Rardin, M. J., He, W., Nishida, Y., Newman, J. C., Carrico, C., Danielson, S. R., Guo, A., Gut, P., Sahu, A. K., Li, B., Uppala, R., Fitch, M., Riiff, T., Zhu, L., Zhou, J., *et al.* (2013) SIRT5 regulates the mitochondrial lysine succinylome and metabolic networks. *Cell Metab.* **18**, 920–933
25. Gaviard, C., Broutin, I., Cosette, P., Dé, E., Jouenne, T., and Hardouin, J. (2018) Lysine succinylation and acetylation in *Pseudomonas aeruginosa*. *J. Proteome Res.* **17**, 2449–2459
26. Wang, J., Li, L., Chai, R., Zhang, Z., Qiu, H., Mao, X., Hao, Z., Wang, Y., and Sun, G. (2019) Succinyl-proteome profiling of *Pyricularia oryzae*, a devastating phytopathogenic fungus that causes rice blast disease. *Sci. Rep.* **9**, 3490
27. Park, J., Chen, Y., Tishkoff, D. X., Peng, C., Tan, M., Dai, L., Xie, Z., Zhang, Y., Zwaans, B. M. M., Skinner, M. E., Lombard, D. B., and Zhao, Y. (2013) SIRT5-mediated lysine desuccinylation impacts diverse metabolic pathways. *Mol. Cell.* **50**, 919–930
28. Wang, G., Xu, L., Yu, H., Gao, J., and Guo, L. (2019) Systematic analysis of the lysine succinylome in the model medicinal mushroom *Ganoderma lucidum*. *BMC Genomics* **20**, 585
29. Zhou, C., Dai, J., Lu, H., Chen, Z., Guo, M., He, Y., Gao, K., Ge, T., Jin, J., Wang, L., Tian, B., Hua, Y., and Zhao, Y. (2019) Succinylome analysis reveals the involvement of lysine succinylation in the extreme resistance of *Deinococcus radiodurans*. *Proteomics* **19**, e1900158
30. Yuan, H., Chen, J., Yang, Y., Shen, C., Xu, D., Wang, J., Yan, D., He, Y., and Zheng, B. (2019) Quantitative succinyl-proteome profiling of Chinese hickory (Carya cathayensis) during the grafting process. *BMC Plant Biol.* **19**, 467
31. Li, X., Hu, X., Wan, Y., Xie, G., Li, X., Chen, D., Cheng, Z., Yi, X., Liang, S., and Tan, F. (2014) Systematic identification of the lysine succinylation in the protozoan parasite *Toxoplasma gondii*. *J. Proteome Res.* **13**, 6087–6095
32. Yang, M., Wang, Y., Chen, Y., Cheng, Z., Gu, J., Deng, J., Bi, L., Chen, C., Mo, R., Wang, X., and Ge, F. (2015) Succinylome analysis reveals the involvement of lysine succinylation in metabolism in pathogenic *Mycobacterium tuberculosis*. *Mol. Cell. Proteomics* **14**, 796–811
33. Kosono, S., Tamura, M., Suzuki, S., Kawamura, Y., Yoshida, A., Nishiyama, M., and Yoshida, M. (2015) Changes in the acetylome and succinylome of *Bacillus subtilis* in response to carbon source. *PLoS One* **10**, e0131169
34. Mizuno, Y., Nagano-Shoji, M., Kubo, S., Kawamura, Y., Yoshida, A., Kawasaki, H., Nishiyama, M., Yoshida, M., and Kosono, S. (2016) Altered acetylation and succinylation profiles in *Corynebacterium glutamicum* in response to conditions inducing glutamate overproduction. *Microbiologyopen* **5**, 152–173
35. Zheng, H., He, Y., Zhou, X., Qian, G., Lv, G., Shen, Y., Liu, J., Li, D., Li, X., and Liu, W. (2016) Systematic analysis of the lysine succinylome in *Candida albicans*. *J. Proteome Res.* **15**, 3793–3801
36. Jin, W., and Wu, F. (2016) Proteome-wide identification of lysine succinylation in the proteins of tomato (Solanum lycopersicum). *PLoS One* **11**, e0147586
37. Shen, C., Xue, J., Sun, T., Guo, H., Zhang, L., Meng, Y., and Wang, H. (2016) Succinyl-proteome profiling of a high taxol containing hybrid *Taxus* species (*Taxus* x media) revealed involvement of succinylation in multiple metabolic pathways. *Sci. Rep.* **6**, 21764
38. Qian, L., Nie, L., Chen, M., Liu, P., Zhu, J., Zhai, L., Tao, S. C., Cheng, Z., Zhao, Y., and Tan, M. (2016) Global profiling of protein lysine malonylation in *Escherichia coli* reveals its role in energy metabolism. *J. Proteome Res.* **15**, 2060–2071
39. Zhang, Y., Wang, G., Song, L., Mu, P., Wang, S., Liang, W., and Lin, Q. (2017) Global analysis of protein lysine succinylation profiles in common wheat. *BMC Genomics* **18**, 309
40. Xu, Y. X., Shen, C. J., Ma, J. Q., Chen, W., Mao, J., Zhou, Y. Y., and Chen, L. (2017) Quantitative succinyl-proteome profiling of *Camellia sinensis* cv. "Anji Baicha" during periodic albinism. *Sci. Rep.* **7**, 1873
41. Xu, X., Liu, T., Yang, J., Chen, L., Liu, B., Wei, C., Wang, L., and Jin, Q. (2017) The first succinylome profile of *Trichophyton rubrum* reveals lysine succinylation on proteins involved in various key cellular processes. *BMC Genomics* **18**, 577
42. Feng, S., Jiao, K., Guo, H., Jiang, M., Hao, J., Wang, H., and Shen, C. (2017) Succinyl-proteome profiling of *Dendrobium officinale*, an important traditional Chinese orchid herb, revealed involvement of succinylation in the glycolysis pathway. *BMC Genomics* **18**, 598
43. Chen, J., Li, F., Liu, Y., Shen, W., Du, X., He, L., Meng, Z., Ma, X., and Wang, Y. (2018) Systematic identification of mitochondrial lysine succinylome in silkworm (*Bombyx mori*) midgut during the larval gluttonous stage. *J. Proteomics* **174**, 61–70
44. Ren, S., Yang, M., Yue, Y., Ge, F., Li, Y., Guo, X., Zhang, J., Zhang, F., Nie, X., and Wang, S. (2018) Lysine succinylation contributes to aflatoxin production and pathogenicity in *Aspergillus flavus*. *Mol. Cell. Proteomics* **17**, 457–471
45. Meng, X., Lv, Y., Mujahid, H., Edelmann, M. J., Zhao, H., Peng, X., and Peng, Z. (2018) Proteome-wide lysine acetylation identification in developing rice (*Oryza sativa*) seeds and protein co-modification by acetylation, succinylation, ubiquitination, and phosphorylation. *Biochim. Biophys. Acta Proteins Proteom.* **1866**, 451–463
46. Henriksen, P., Wagner, S. A., Weinert, B. T., Sharma, S., Bačinskaja, G., Rehman, M., Juffer, A. H., Walther, T. C., Lisby, M., and Choudhary, C. (2012) Proteome-wide analysis of lysine acetylation suggests its broad regulatory scope in saccharomyces cerevisiae. *Mol. Cell. Proteomics* **11**, 1510–1522
47. Harmel, R., and Fiedler, D. (2018) Features and regulation of non-enzymatic post-translational modifications. *Nat. Chem. Biol.* **14**, 244–252
48. Klausen, M. S., Jespersen, M. C., Nielsen, H., Jensen, K. K., Jurtz, V. I., Sønderby, C. K., Sommer, M. O. A., Winther, O., Nielsen, M., Petersen, B., and Marcatili, P. (2019) NetSurfP-2.0: Improved prediction of protein structural features by integrated deep learning. *Proteins* **87**, 520–527
49. Ramachandran, G. N., Ramakrishnan, C., and Sasisekharan, V. (1963) Stereochemistry of polypeptide chain configurations. *J. Mol. Biol.* **7**, 95–99
50. Armenteros, J. J. A., Salvatore, M., Emanuelsson, O., Winther, O., von Heijne, G., Elofsson, A., and Nielsen, H. (2019) Detecting sequence signals in targeting peptides using deep learning. *Life Sci. Alliance.* **2**, e201900429
51. Gao, J., and Xu, D. (2011) Correlation between posttranslational modification and intrinsic disorder in protein. *Biocomput* **2012**, 94–103
52. Oldfield, C. J., and Dunker, A. K. (2014) Intrinsically disordered proteins and intrinsically disordered protein regions. *Annu. Rev. Biochem.* **83**, 553–584
53. Miyakawa, I. (2017) Organization and dynamics of yeast mitochondrial nucleoids. *Proc. Jpn. Acad. Ser. B.* **93**, 339–359
54. Vozáriková, V., Kunová, N., Bauer, J. A., Frankovský, J., Kotrasová, V., Procházková, K., Džugasová, V., Kutejová, E., Pevala, V., Nosek, J., and Tomáška, Ľ. (2020) Mitochondrial HMG-box containing proteins: From biochemical properties to the roles in human diseases. *Biomolecules* **10**, 1193
55. Dilweg, I. W., and Dame, R. T. (2018) Post-translational modification of nucleoid-associated proteins: An extra layer of functional modulation in bacteria? *Biochem. Soc. Trans.* **46**, 1381–1392
56. Ho, B., Baryshnikova, A., and Brown, G. W. (2018) Unification of protein abundance datasets yields a quantitative *Saccharomyces cerevisiae* proteome. *Cell Syst* **6**, 192–205.e3
57. Kaufman, B. A., Newman, S. M., Hallberg, R. L., Slaughter, C. A., Perlman, P. S., and Butow, R. A. (2000) *In organello* formaldehyde crosslinking of proteins to mtDNA: Identification of bifunctional proteins. *Proc. Natl. Acad. Sci. U. S. A.* **97**, 7772–7777
58. Chakraborty, A., Lyonnais, S., Battistini, F., Hospital, A., Medici, G., Prohens, R., Orozco, M., Vilardell, J., and Soì, M. (2016) DNA structure directs positioning of the mitochondrial genome packaging protein Abf2p. *Nucleic Acids Res.* **45**, 951–967
59. Li, Y., Li, H., Sui, M., Li, M., Wang, J., Meng, Y., Sun, T., Liang, Q., Suo, C., Gao, X., Li, C., Li, Z., Du, W., Zhang, B., Sai, S., *et al.* (2019) Fungal acetylome comparative analysis identifies an essential role of acetylation in human fungal pathogen virulence. *Commun. Biol.* **2**, 154
60. Paik, W. K., Pearson, D., Lee, H. W., and Kim, S. (1970) Nonenzymatic acetylation of histones with acetyl-CoA. *Biochim. Biophys. Acta* **213**, 513–522

61. Wolfe, A. J. (2016) Bacterial protein acetylation: New discoveries unanswered questions. *Curr. Genet.* **62**, 335–341
62. Čanigová, N. (2017) *Comparative Analysis of Mitochondrial HMG Box-Containing Proteins*. M.Sc. Thesis, Comenius University in Bratislava
63. Miyakawa, I., Okamuro, A., Kinsky, S., Visacka, K., Tomaska, L., and Nosek, J. (2009) Mitochondrial nucleoids from the yeast *Candida parapsilosis*: Expansion of the repertoire of proteins associated with mitochondrial DNA. *Microbiology* **155**, 1558–1568
64. Višacká, K., Gerhold, J. M., Petrovičová, J., Kinský, S., Jõers, P., Nosek, J., Sedman, J., and Tomáška, Ľ. (2009) Novel subfamily of mitochondrial HMG box-containing proteins: Functional analysis of Gcf1p from *Candida albicans*. *Microbiology* **155**, 1226–1240
65. Bakkaiová, J., Arata, K., Matsunobu, M., Ono, B., Aoki, T., Lajdova, D., Nebohacova, M., Nosek, J., Miyakawa, I., and Tomaska, L. (2014) The strictly aerobic yeast *Yarrowia lipolytica* tolerates loss of a mitochondrial DNA-packaging protein. *Eukaryot. Cell.* **13**, 1143–1157
66. Crooks, D. R., Maio, N., Lang, M., Ricketts, C. J., Vocke, C. D., Gurram, S., Turan, S., Kim, Y. Y., Cawthon, G. M., Sohelian, F., De Val, N., Pfeiffer, R. M., Jailwala, P., Tandon, M., Tran, B., *et al.* (2021) Mitochondrial DNA alterations underlie an irreversible shift to aerobic glycolysis in fumarate hydratase-deficient renal cancer. *Sci. Signal.* **14**, eabc4436
67. Yang, M., Ternette, N., Su, H., Dabiri, R., Kessler, B., Adam, J., Teh, B., and Pollard, P. (2014) The succinated proteome of FH-mutant tumours. *Metabolites* **4**, 640–654
68. Kunová, N., Ondrovičová, G., Bauer, J. A., Bellová, J., Ambro, L., Martináková, L., Kotrasová, V., Kutejová, E., and Pevala, V. (2017) The role of Lon-mediated proteolysis in the dynamics of mitochondrial nucleic acid-protein complexes. *Sci. Rep.* **7**, 631
69. Gao, W., Wu, M., Wang, N., Zhang, Y., Hua, J., Tang, G., and Wang, Y. (2018) Increased expression of mitochondrial transcription factor a and nuclear respiratory factor-1 predicts a poor clinical outcome of breast cancer. *Oncol. Lett.* **15**, 1449–1458
70. Xie, Z., Dai, J., Dai, L., Tan, M., Cheng, Z., Wu, Y., Boeke, J. D., and Zhao, Y. (2012) Lysine succinylation and lysine malonylation in histones. *Mol. Cell. Proteomics* **11**, 100–107
71. Wang, Y., Guo, Y. R., Liu, K., Yin, Z., Liu, R., Xia, Y., Tan, L., Yang, P., Lee, J. H., Li, X. J., Hawke, D., Zheng, Y., Qian, X., Lyu, J., He, J., *et al.* (2017) KAT2A coupled with the α-KGDH complex acts as a histone H3 succinyltransferase. *Nature* **552**, 273–277
72. Dehzangi, A., López, Y., Lal, S. P., Taherzadeh, G., Sattar, A., Tsunoda, T., and Sharma, A. (2018) Improving succinylation prediction accuracy by incorporating the secondary structure via helix, strand and coil, and evolutionary information from profile bigrams. *PLoS One* **13**, e0191900
73. Ondrovičová, G., Liu, T., Singh, K., Tian, B., Li, H., Gakh, O., Perečko, D., Janata, J., Granot, Z., Orly, J., Kutejová, E., and Suzuki, C. K. (2005) Cleavage site selection within a folded substrate by the ATP-dependent Lon protease. *J. Biol. Chem.* **280**, 25103–25110
74. Bennett, B. D., Kimball, E. H., Gao, M., Osterhout, R., Van Dien, S. J., and Rabinowitz, J. D. (2009) Absolute metabolite concentrations and implied enzyme active site occupancy in *Escherichia coli*. *Nat. Chem. Biol.* **5**, 593–599
75. Di Bartolomeo, F., Malina, C., Campbell, K., Mormino, M., Fuchs, J., Vorontsov, E., Gustafsson, C. M., and Nielsen, J. (2020) Absolute yeast mitochondrial proteome quantification reveals trade-off between biosynthesis and energy generation during diauxic shift. *Proc. Natl. Acad. Sci. U. S. A.* **117**, 7524–7535
76. Chen, X. J., and Butow, R. A. (2005) The organization and inheritance of the mitochondrial genome. *Nat. Rev. Genet.* **6**, 815–825
77. Gibson, G. E., Xu, H., Chen, H.-L., Chen, W., Denton, T. T., and Zhang, S. (2015) Alpha-ketoglutarate dehydrogenase complex-dependent succinylation of proteins in neurons and neuronal cell lines. *J. Neurochem.* **134**, 86–96
78. Valachovič, M., Bareither, B. M., Bhuiyan, M. S. A., Eckstein, J., Barbuch, R., Balderes, D., Wilcox, L., Sturley, S. L., Dickson, R. C., and Bard, M. (2006) Cumulative mutations affecting sterol biosynthesis in the yeast *Saccharomyces cerevisiae* result in synthetic lethality that is suppressed by alterations in sphingolipid profiles. *Genetics* **173**, 1893–1908
79. Gietz, R. D., Schiestl, R. H., Willems, A. R., and Woods, R. A. (1995) Studies on the transformation of intact yeast cells by the LiAc/SS-DNA/PEG procedure. *Yeast* **11**, 355–360
80. Nosek, J., and Tomáška, Ľ. (2013) *Laboratory Protocols in Molecular and Cell Biology of Yeasts*, Create Space Independent Publishing Platform, Create Space Independent Publishing Platform, Charleston, SC
81. Van Dijl, J. M., Kutejová, E., Suda, K., Perečko, D., Schatz, G., and Suzuki, C. K. (1998) The ATPase and protease domains of yeast mitochondrial Lon: Roles in proteolysis and respiration-dependent growth. *Proc. Natl. Acad. Sci. U. S. A.* **95**, 10584–10589
82. Suzuki, C. K., Kutejová, E., and Suda, K. (1995) Analysis and purification of ATP-dependent mitochondrial Lon protease of *Saccharomyces cerevisiae*. *Methods Enzymol.* **260**, 486–494
83. Somogyi, M. (1952) Notes on sugar determination. *J. Biol. Chem.* **195**, 19–23
84. Michalski, A., Damoc, E., Lange, O., Denisov, E., Nolting, D., Müller, M., Viner, R., Schwartz, J., Remes, P., Belford, M., Dunyach, J. J., Cox, J., Horning, S., Mann, M., and Makarov, A. (2012) Ultra high resolution linear ion trap orbitrap mass spectrometer (orbitrap elite) facilitates top down LC MS/MS and versatile peptide fragmentation modes. *Mol. Cell. Proteomics* **11**. O111.013698
85. Cox, J., and Mann, M. (2008) MaxQuant enables high peptide identification rates, individualized p.p.b.-range mass accuracies and proteome-wide protein quantification. *Nat. Biotechnol.* **26**, 1367–1372
86. Morgenstern, M., Stiller, S. B., Lübbert, P., Peikert, C. D., Dannenmaier, S., Drepper, F., Weill, U., Höß, P., Feuerstein, R., Gebert, M., Bohnert, M., van der Laan, M., Schuldiner, M., Schütze, C., Oeljeklaus, S., *et al.* (2017) Definition of a high-confidence mitochondrial proteome at quantitative scale. *Cell Rep.* **19**, 2836–2852
87. Vögtle, F. N., Burkhart, J. M., Gonczarowska-Jorge, H., Kücükköse, C., Taskin, A. A., Kopczynski, D., Ahrends, R., Mossmann, D., Sickmann, A., Zahedi, R. P., and Meisinger, C. (2017) Landscape of submitochondrial protein distribution. *Nat. Commun.* **8**, 1–10
88. Mi, H., Muruganujan, A., Ebert, D., Huang, X., and Thomas, P. D. (2019) PANTHER version 14: More genomes, a new PANTHER GO-slim and improvements in enrichment analysis tools. *Nucleic Acids Res.* **47**, D419–D426
89. Balakrishnan, R., Park, J., Karra, K., Hitz, B. C., Binkley, G., Hong, E. L., Sullivan, J., Micklem, G., and Cherry, J. M. (2012) YeastMine-An integrated data warehouse for *Saccharomyces cerevisiae* data as a multipurpose tool-kit. *Database* **2012**, bar062
90. Cherry, J. M., Hong, E. L., Amundsen, C., Balakrishnan, R., Binkley, G., Chan, E. T., Christie, K. R., Costanzo, M. C., Dwight, S. S., Engel, S. R., Fisk, D. G., Hirschman, J. E., Hitz, B. C., Karra, K., Krieger, C. J., *et al.* (2012) Saccharomyces Genome Database: The genomics resource of budding yeast. *Nucleic Acids Res.* **40**, D700–D705
91. Crooks, G. E., Hon, G., Chandonia, J. M., and Brenner, S. E. (2004) WebLogo: A sequence logo generator. *Genome Res.* **14**, 1188–1190
92. Thomsen, M. C. F., and Nielsen, M. (2012) Seq2Logo: A method for construction and visualization of amino acid binding motifs and sequence profiles including sequence weighting, pseudo counts and two-sided representation of amino acid enrichment and depletion. *Nucleic Acids Res.* **40**, W281–W287
93. Bakkaiová, J., Marini, V., Willcox, S., Nosek, J., Griffith, J. D., Krejci, L., and Tomáška, Ľ. (2016) Yeast mitochondrial HMG proteins: DNA-binding properties of the most evolutionarily divergent component of mitochondrial nucleoids. *Biosci. Rep.* **36**, e00288
94. Bradford, M. (1976) A rapid and sensitive method for the quantitation of microgram quantities of protein utilizing the principle of protein-dye binding. *Anal. Biochem.* **72**, 248–254
95. Green, M. R., and Sambrook, J. (2012) *Molecular Cloning: A Laboratory Manual*, Cold Spring Harbor Laboratory Press, New York, NY
96. Berrow, N. S., Alderton, D., Sainsbury, S., Nettleship, J., Assenberg, R., Rahman, N., Stuart, D. I., and Owens, R. J. (2007) A versatile ligation-independent cloning method suitable for high-throughput expression screening applications. *Nucleic Acids Res.* **35**, e45
97. Du, J., Zhou, Y., Su, X., Yu, J. J., Khan, S., Jiang, H., Kim, J., Woo, J., Kim, J. H., Choi, B. H., He, B., Chen, W., Zhang, S., Cerione, R. A., Auwerx, J.,

et al. (2011) Sirt5 is a NAD-dependent protein lysine demalonylase and desuccinylase. *Science* **334**, 806–809
98. Kovalevskiy, O., Nicholls, R. A., Long, F., Carlon, A., and Murshudov, G. N. (2018) Overview of refinement procedures within REFMAC 5: Utilizing data from different sources. *Acta Crystallogr. Sect. D Struct. Biol.* **74**, 215–227
99. Case, D. A., Babin, V., Berryman, J. T., Betz, R. M., Cai, Q., Cerutti, D. S., Cheatham, T. E., III, Darden, T. A., Duke, R. E., Gohlke, H., Goetz, A. W., Gusarov, S., Homeyer, N., Janowski, P., Kaus, J., *et al.* (2014) *AMBER 14*, University of California, San Francisco, San Francisco, CA
100. Pettersen, E. F., Goddard, T. D., Huang, C. C., Couch, G. S., Greenblatt, D. M., Meng, E. C., and Ferrin, T. E. (2004) UCSF Chimera - a visualization system for exploratory research and analysis. *J. Comput. Chem.* **25**, 1605–1612
101. Williams, C. J., Headd, J. J., Moriarty, N. W., Prisant, M. G., Videau, L. L., Deis, L. N., Verma, V., Keedy, D. A., Hintze, B. J., Chen, V. B., Jain, S., Lewis, S. M., Arendall, W. B., Snoeyink, J., Adams, P. D., *et al.* (2018) MolProbity: More and better reference data for improved all-atom structure validation. *Protein Sci.* **27**, 293–315
102. Jurrus, E., Engel, D., Star, K., Monson, K., Brandi, J., Felberg, L. E., Brookes, D. H., Wilson, L., Chen, J., Liles, K., Chun, M., Li, P., Gohara, D. W., Dolinsky, T., Konecny, R., *et al.* (2018) Improvements to the APBS biomolecular solvation software suite. *Protein Sci.* **27**, 112–128
103. Perez-Riverol, Y., Csordas, A., Bai, J., Bernal-Llinares, M., Hewapathirana, S., Kundu, D. J., Inuganti, A., Griss, J., Mayer, G., Eisenacher, M., Pérez, E., Uszkoreit, J., Pfeuffer, J., Sachsenberg, T., Yilmaz, Ş., *et al.* (2019) The PRIDE database and related tools and resources in 2019: Improving support for quantification data. *Nucleic Acids Res.* **47**, D442–D450
104. Schneider, C. A., Rasband, W. S., and Eliceiri, K. W. (2012) NIH image to ImageJ: 25 years of image analysis. *Nat. Methods* **9**, 671–675
105. Stringer, C., Wang, T., Michaelos, M., and Pachitariu, M. (2021) Cellpose: a generalist algorithm for cellular segmentation. *Nat. Methods* **18**, 100–106